ELECTRODEPOSICIÓN DE MATERIALES COMPUESTOS APLICADOS A TERMOACTUADORES

Tutora España: Elisa Ruiz Navas
Tutor Bélgica: Jan Fransaer
Contacto Bélgica: Linda Stappers
Autor: Jesús La Parra Albaladejo

Table of contents

Acknowledgements

I would like to thank Professor Jan Fransaer and Linda Stappers for helping me during these months with their advises and teachings in order to finish the present experimental work.

Without their help, this thesis could not be finished.
Thanks for their understanding as I have had to visit Spain several times in order to make exams for finishing my studies.

I am also grateful to An Kempeneers, Marc Peeters and Danny Winant for lending me all the devices and material I have needed during the realization of the experiments and for doing the tests for completing my daily work.

I would like to express my most sincere thanks also to Martine Wevers and Huberte Cloosen for their administration during my whole academic year here in Leuven. And also to my Erasmus coordinator in Spain, Elisa Ruiz Navas.

Finally, I would like to express my gratitude to my family, to my friends here in Leuven and in Spain and to my home mate during this year.

List of symbols

a : particle radius

b : metal matrix radius

D : cylinders radius

E : elastic modulus (GPa)

f : particle concentration in volume %

G : shear modulus (GPa)

I : current (A)

k : thermal conductivity (W/mK)

K : bulk modulus (GPa)

p : pressure (Pa)

R : elastic metal matrix radius

Re : Reynolds number

S : area (m^2)

t : time (s)

u: displacement (m)

T : temperature (ºC)

V : volume (m_3)

α : thermal expansion coefficient ($ºC^{-1}$)

ε : strain

v : kinematic viscosity (m^2/s)

ρ : density (kg/m^3)

σ : stress (MPa)

σ_r: radial stress (MPa)

σ_t: tangential stress (MPa)

σ_0 : yield stress (MPa)

ω : rotational speed (rpm)

Chapter 1: *Introduction*

The aim of this Master Thesis is to analyse the thermal and mechanical properties of composite materials made up of a metal matrix (nickel and copper) and polymer particles finely and homogeneously embedded on it (solid polystyrene and microcapsules containing water).

The main focus of study will be the expansion behaviour arising from the phase change of the particles embedded in the metal matrix in a small temperature range and its relationship to the change in the elastic modulus.
It is expected that the resultant thermal expansion coefficient rises because of the higher values of these particles embedded on the metal matrix. In the case of PS particles, the thermal expansion coefficient varies from $90 \cdot 10^{-6}$ to $150 \cdot 10^{-6}$ $ºC^{-1}$ whereas for copper and nickel at room temperature is $16.5 \cdot 10^{-6}$ and $13.4 \cdot 10^{-6}$ respectively. The thermal expansion obtained is expected to be higher in the copper coatings as it has lower elastic modulus, 115 GPa for copper and 207 GPa for nickel, and lower yield strength, varying from 18 to 69 MPa in the case of electrodeposited copper and from 35 to 107 MPa for electrodeposited nickel.[1]

This expansion behaviour under thermal loads, with a sharp rise in a small temperature range, will be responsible for their applicability in fields such as thermo actuators.

Each material separately does not have such adequate properties for being used as thermo actuators. On the one hand, metals have a high thermal conductivity coefficient (398 W/mK and 90 W/mk for copper and nickel respectively) but a low thermal storage capacity (386 J/kgK and 443 J/kgK for copper and nickel respectively) so they suffer thermal fatigue when heating cycles are applied reducing their life time due to the thermal stresses. On the other hand, the particles used have a poor thermal conductivity (0.13 W/mK for PS) and therefore their response to temperature changes is slowly performed. The particles have a high thermal storage capacity (1170 J/kgK and 4180 J/kgK for PS and water respectively) and therefore they will absorb part of the thermal stresses avoiding the premature degradation of the samples.[2]

In order to analyse the properties above mentioned, some tests must be carried out such as differential scanning calorimetry (DSC) and thermal dilatometry, which will be explained in detail in chapter 4.

In order to perform thermal dilatometry, cylindrical samples are required. They were prepared by electrocodeposition by using parallel anode and rotating cylinder cathode (RCC). Agitation was applied during experiments. The complete process will be explained in chapter 3.

Chapter 2: *Literature review*

2.1 Microencapsulation techniques

Phase change material microcapsules are spherical substances with a core and shell structure, where the core consists in a phase change material (PCM) enwrapped by a protective shell material.

The phase change materials can absorb and release heat from their surroundings in dynamic heat exchange processes when they reach their melting point or their crystallization temperature in the case of polymer materials.

In order to produce the microcapsules core, several PCMs can be used, such as linear chain hydrocarbons known as paraffin waxes, hydrated salts, polyethylene glycols, fatty acids and mixture of eutectics of organic and non-organic compounds. In the present work, water and polystyrene will be used as PCM.[3]

The microcapsules are defined with several parameters such as their particle diameter, the thickness of shell, the thermal storage capacity and conductivity, durability, etc. The thickness of the particle walls may be less than 1 μm, and the particle sizes vary within the range of less than 1 μm to more than 300 μm depending on the method of encapsulation used, typically between 10 and 40 μm in diameter. The PCM content of the capsules may be up to 80 - 85 %.

The microencapsulation process depends on several parameters such as stirring speed, temperature, duration, pH of the reaction mixture, contents of emulsification agent.

The microcapsules production may be achieved by physical or chemical techniques. The use of some techniques has been limited due to the high costs of processing, regulatory affairs, and the use of organic solvents, which are a hazard for the human health and the environment and make difficult their recycling.[4]

2.1.1 Physical methods

They are mainly spray drying or centrifugal and fluidized bed processes, which are inherently not capable of producing microcapsules smaller than 100 μm.

- *Spray drying process:* an emulsion containing the core material, consisting in oil or a liquid immiscible in water, is dispersed into a concentrated solution of the shell material until the desired size of oil droplets is obtained. Then the resultant mixture is atomized into spray by using a rotating disc. Microcapsules are developed by dehydration when the spray droplets touch the heated walls of the drying chamber.
  This method is usually applied in the alimentary, pharmaceutical and chemical industries.
- *Centrifugal process:* two immiscible solutions containing the core and the shell materials are expulsed through a double spinning nozzle. The droplets come in contact and shell is solidified either by cooling or by a gelling bath.
- *Fluidized bed coating process:* it is used for encapsulating solid core materials or liquids absorbed by porous solids by suspending them on an air jet and then by covering those with a liquid spray coating. Then the shell is solidified by solvent evaporation or cooling.

2.1.2 Chemical methods

The chemical methods are more suitable for producing microcapsules. The processes are associated with the simple or complex coacervation and interfacial or in situ polymerization techniques.

- *Coacervation process:* it is a colloidal process in which the core material in a dispersed form is added to the polymer solution. Then the mixture is suspended in an aqueous phase containing a surface–active agent. Microencapsulation of both oily and water–soluble actives is possible by using oil–in–water and water–in–oil techniques. As oil–in–water coacervation is more straightforward, it is widely used in the industry. The process can be simple or complex coacervation depending on the number of colloids used.
  Encapsulation of paraffin waxes by complex coacervation was succeeded in other experiments in order to obtain a high energy storage/release capacity of about 170–220 kJ/kg for being used as a solar energy storage material. The main limitation of this approach is the difficulty in scale up the process from the laboratory to the industry.
- *Interfacial polymerization process:* it involves bringing together two immiscible liquids, such as water and organic solvents, containing complimentary, direct-acting, organic intermediates that will react with each other in order to form a solid pre-condensate. Condensation polymers are usually formed by the stepwise intermolecular condensation of reactive groups. The structural units of condensation polymers are usually joined by inter-unit functional groups. The in situ processes have the ability to yield microcapsules with the best quality in terms of diffusion–tightness of their walls and of a size ranging between 5 and 100 μm. Suitable polymers such as a polyamide, polyester, polyurethane, polyurea or polystyrene, can be formed from resin intermediates or monomers.
- *In situ polymerization process:* it is very similar to the interfacial polymerization except that no reactants are used.[5]

2.2 Electrodeposition technique

The composite electrodeposition consists in particle incorporation during the electrolytic deposition of metal in the cathode. As a result, a composite coating composed by a metal matrix and a dispersion of particles of ceramics, metals or organic compounds is developed.

The advantages of composite electrodeposition over other coatings methods are the possibility of being continuously performed and at standard conditions. As a consequence this method avoids the problems associated with different factors such as high temperature and pressure processing, uniformity of deposition and particle distribution even in complex shapes, reduction of waste, low levels of contamination of the samples and the ability to produce functionally-gradient material.

Several variables, most of them interrelated, influence the process:

- *Hydrodynamics*: electrolyte agitation is needed to maintain the particles in suspension and to transport them to the surface of the cathode being incorporated in the metal matrix.
  Therefore, an increase in flow can enlarge the deposition rate. However, if the agitation is too intense, the residence time of the particles in the cathode surface is not sufficient and they are swept away before being incorporated in the matrix.
  A PFTE paddle stirrer is mounted at the end of the rotating cylinder cathode (RCC) in order to enhance the agitation of the bath at 300 rpm.
  The electrodeposition is performed using parallel anode configuration due to its simplicity and uniform current density. The flow in the concentric RCC cell is turbulent if Reynolds number is between 100-200, enhancing the deposition rate and avoiding the movement in concentric circles typical of laminar flow.

$$\mathrm{Re} = \frac{\omega\left(\frac{D}{2}\right)^2}{\nu} = \frac{\frac{2\pi}{60}300 \cdot 2.3 \cdot 10^{-3}}{10^{-6}} = 166.19 \longrightarrow \text{turbulent flow} \qquad (2.1)$$

where, Re is the Reynolds number, ω the rotating speed (rad/s), D the cylinder diameter and ν the kinematic viscosity (m^2/s).

- *Current density*: it determines the time required to achieve the desired coating thickness and affects the particles deposition rate. If the current density is too high, the deposition of metal ion is accelerated and the incorporation of particles in the metal matrix is reduced as a consequence of their bigger size and weight. It is thus necessary to find equilibrium between the particles deposition rate and the time spent in the electrodeposition.
  In the case of copper and nickel coatings containing particles, the applied current density is 2 A/dm^2, while the pure nickel coating were carried out at 5 A/dm^2.
- *Particles characteristics*: electrodeposition depends on composition, size, density, shape and surface properties (stickiness provoking agglomerates, surface charge, uniformity…) of particles to be incorporated in the metal matrix.
  The microcapsules containing water have a main size of 22 μm and the solid polystyrene of 4 μm, being both of them spherical.
- *Bath composition*: it is determined by the type and concentration of electrolyte, the pH (due to the embrittlement provoked by the hydrogen in the coatings), the particles concentration in suspension (in our case 300, 200 and 100 g/l, for higher values settlement can occur), the temperature (room temperature for copper coatings and 55 ºC for nickel coatings) and the presence of additives (such as surfactants).[6]

2.3 Laser diffraction particle sizing

In order to measure the particle sizes produced during the experiments, the laser diffraction technique is used. It is based on the principle that particles passing through a laser beam will scatter light at an angle directly related to their size. As the particle size decreases, the observed scattering angle increases logarithmically. The observed scattering intensity is also dependent on particle sizes and it is reduced in relation to the particle's cross-sectional area. Large particles therefore scatter light at narrow angles with high intensity whereas small particles scatter at wider angles but with lower intensity.
A typical device consists of:

- A laser, to provide a source of coherent, intense light of fixed wavelength
- A sample system to ensure that material under test passes through the laser beam as a homogeneous stream of particles in a known and reproducible state of dispersion
- A series of detectors which are used to measure the light pattern produced over a wide range of angles.

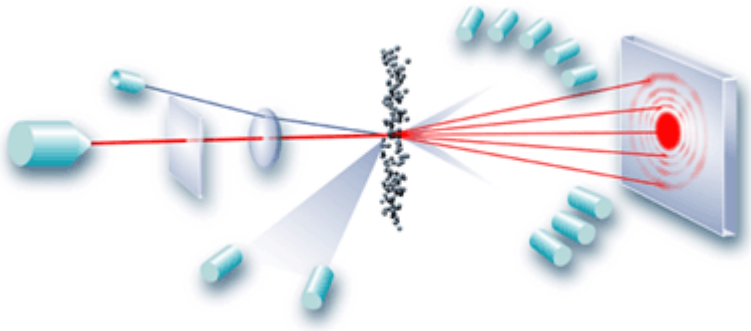

Figure 2.1 Laser diffraction scheme

The size range accessible during the measurement is directly related to the angular range of the scattering measurement from around 0.02 degrees to 130 degrees. A logarithmic detector sequence can measure small angles when the detectors are grouped close together. If wider angles need to be measured, the detector will become more widely spaced. This makes possible to detect the changes in scattering angle observed even when the particle size decreases. The detector sequence is generally set up such that equal volumes of particles of different sizes produce a similar measured signal.

In laser diffraction, particle size distributions are calculated by comparing a sample's scattering pattern with an appropriate optical model using a mathematical inversion process. Two different models are traditionally used: the Fraunhofer approximation, which is simpler and only accurate in measuring particle sizes above 50 microns, and the Mie Theory, more accurate and suitable for smaller particle sizes.

The Mie Theory provides a rigorous solution for the calculation of particle size distributions from light scattering data and is based on the Maxwell's electromagnetic field equations.

Moreover, it predicts scattering intensities for all particles, either small or large, as well as transparent or opaque following several assumptions:

- The particles being measured are spherical
- The suspension is dilute; as a result, the scattered light is measured before it is re-scattered by other particles
- The optical properties of the particles and the medium surrounding them are both known
- The particles are homogeneous

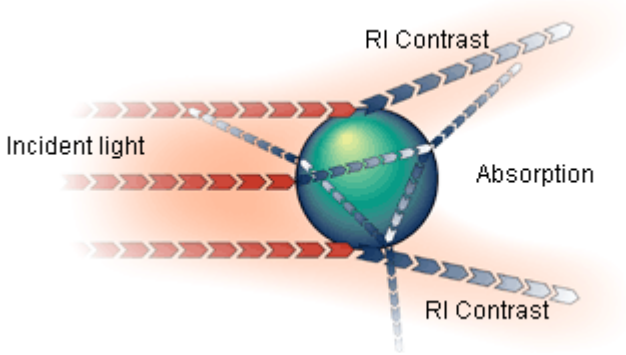

Figure 2.2 Particle - light interaction

The Mie Theory predicts the primary scattering response observed from the surface of the particle, with the intensity predicted by the refractive index difference between the particle and the dispersion medium. It also predicts how the particle's absorption affects

the secondary scattering signal caused by light refraction within the particle (this is especially important for particles with diameters below 50 microns and for transparent particles).

The main aim of all particle-sizing techniques is to provide a single representative number of the particle size. However, as particles are three-dimensional objects, at least three parameters (length, breadth and height) are required in order to provide a complete description. Therefore, most sizing techniques assume that the material being measured is spherical and refer to the particle size as the diameter of the "equivalent sphere" which would give the same response as the particle being measured.[7]

Once the particle size of the measured sample has been calculated, the distribution of particle sizes is displayed as shown in Chapter 3

Chapter 3: *Experimental work*

3.1 Synthesis of particles

3.1.1 Preparation of microcapsules containing water

The microcapsules were obtained by mixing 3 batches, each one composed at the same time by 3 different solutions A, B and C.

- 100 ml of a 4 wt. % solution of gelatine in water (solution A)
  Mixed at 40 °C with a magnetic stirrer
- 140 ml of a 5 wt. % solution of polystyrene in dichloromethane (solution B)
  Mixed with a magnetic stirrer at room temperature to avoid dichloromethane evaporation
- 500 ml of a 1 wt. % solution of gelatine in water (solution C)
  Mixed at 40 °C with a magnetic stirrer

The emulsification of microcapsules consisted in several steps. First, solution A was added to solution B while vigorously stirring with an Ultra-Turrax at 8000 rpm during 15 minutes at room temperature in order to obtain solution D. The resultant product was then added to solution C while vigorously stirring with a second Ultra-Turrax at 8000 rpm during 1 minute below room temperature by using ice to cool the solution in order to reduce the particles size.

Figure 3.1 Ultra-Turrax used during microcapsules and solid polystyrene particles emulsification

In the meanwhile, another batch of solution C was agitated with a paddle stirrer at 1500 rpm in a double walled beaker maintaining a constant temperature of 15 ºC with a thermostatic bath. As soon as the mixture of solution D and solution C was ready, it was immediately poured into the beaker containing the solution C.

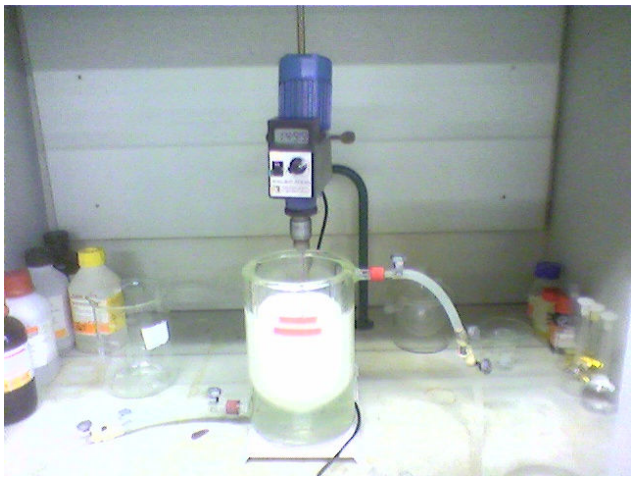

Figure 3.2 Paddle stirrer and double wall beaker used during dichloromethane evaporation

These steps were repeated three times, once for each batch. When the three batches were put together in the beaker, they continued being agitated at 1500 rpm at 15ºC during 20 minutes. The temperature was a key issue and must be maintained below room temperature for controlling the particles size distribution.

When the 20 minutes had passed, the stirring speed was lowered to 250 rpm and the temperature risen to 30 ºC.
In order to evaporate the dichloromethane, temperature was increased 5 ºC each 15 minutes until 50 ºC is reached. The complete evaporation lasted 16 hours.

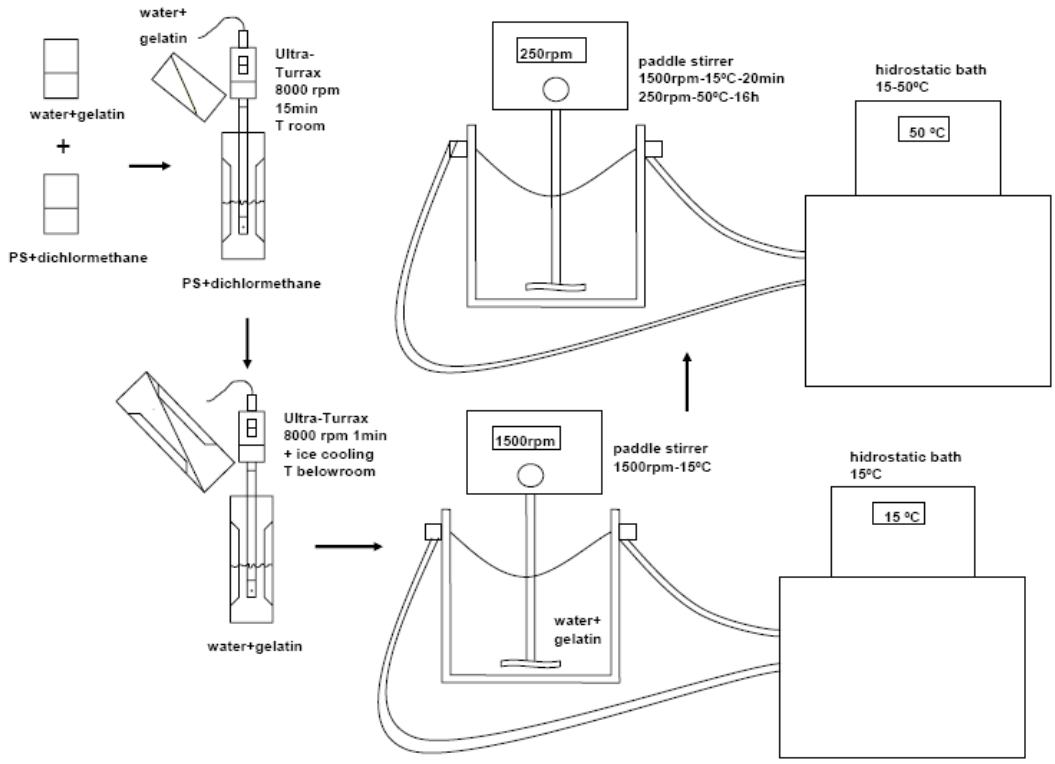

Figure 3.3 Scheme of the synthesis of the microcapsules

Once the microcapsules were obtained, they must be washed. First, microcapsules were settled by repeated centrifugation at 10000 rpm during 6 minutes using a centrifugation machine (Hettich Zentrifugen Rotina 35). Then, they were washed during 15-20 minutes in water at 50 °C while agitating with a paddle stirrer at 400 rpm.

Figure 3.4 Centrifugation machine used for particles settling

After each washing, the conductivity of the water obtained after centrifugation was measured in order to find out if the particles were completely clean (when it reaches a value around 2 μS/cm). The values obtained were:

1st washing 525 μS/cm
2nd washing 75.5 μS/cm
3rd washing 8.3 μS/cm
4th washing 6.5 μS/cm
5th washing 4.1 μS/cm
6th washing 3.3 μS/cm
7th washing 2.7 μS/cm

The microcapsule size distribution was obtained by using a laser diffraction particle sizing machine (Mastersizer Malvern Instruments).

Figure 3.5 Mastersizer machine for particle size measurement

The way it works is explained in Chapter 2. The main size achieved was around 22 μm:

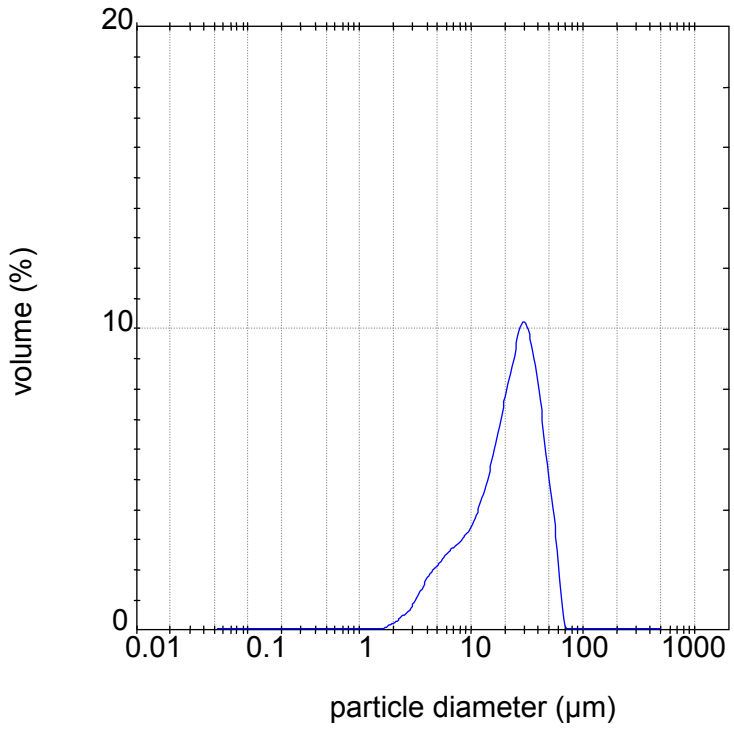

Figure 3.6 Distribution of the microcapsules sizes

3.1.2. Preparation of solid polystyrene particles

The PS particles were obtained by mixing 3 batches. Each one was composed at the same time by 3 different solutions A, B and C.

- 400 ml of a 1 wt. % solution of gelatine in water (solution A)
  Mixed at 40 °C with a magnetic stirrer
- 300 ml of a 6.7 wt. % solution of polystyrene in dichloromethane (solution B)
  Mixed at room temperature with a magnetic stirrer
- 600 ml of a 1 wt. % solution of gelatine in water (solution C)
  Mixed at 40 °C with a magnetic stirrer

The emulsification of solid polystyrene particles consisted in several steps. First, solution A was added to solution B while vigorously stirring with an Ultra-Turrax at 20000 rpm for 1 minute at room temperature in order to obtain solution D.

In the meanwhile, solution C was agitated with a paddle stirrer at 1500 rpm in a double walled beaker at room temperature. As soon as the mixture of solution D and solution C was ready, it was immediately poured into the beaker containing the solution C.

These steps were repeated three times, one for each batch. When the three batches were put together in the beaker, they continued being agitated at 1500 rpm at 30 ºC during 30 minutes. In this case, the condition of temperature below room temperature was no longer necessary.

Once the 30 minutes passed, the stirring speed was lowered to 250 rpm and the temperature was risen 5 ºC each 15 minutes until 50 ºC was reached in order to evaporate the dichloromethane. The complete evaporation lasted 16 hours.

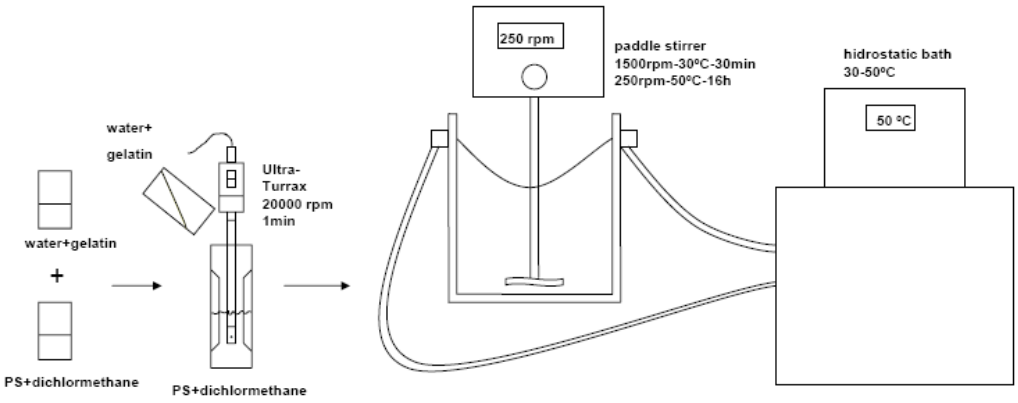

Figure 3.7 Scheme of the synthesis of the PS particles

Once the solid polystyrene particles were obtained, they must be washed in the same way as microcapsules. The conductivity values obtained after each washing were:

1st washing 1143 μS/cm
2nd washing 92 μS/cm
3rd washing 5.7 μS/cm
4th washing 2.5 μS/cm
5th washing 2.4 μS/cm
6th washing 1.9 μS/cm

The particle main size was measured in the same way as microcapsules, being around 4 μm:

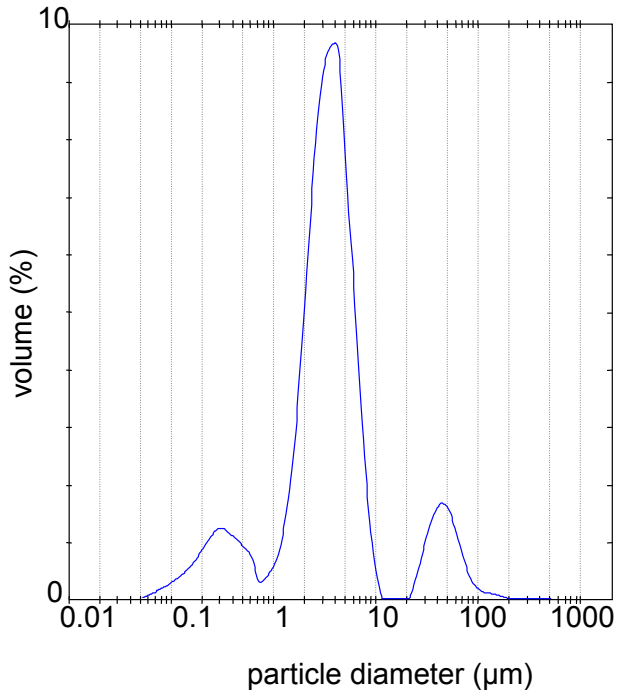

Figure 3.8 Distribution of the solid polystyrene particles sizes

3.2 Synthesis of composite coatings

In the following table the different coatings developed during the experimental work can be found as well as their principal characteristics, such as the temperature and the current density applied during the electrodeposition process, the particles concentration in the bath, the carbon content in weight and the volume fraction of particles contained in each sample. In order to calculate the latter parameter, the carbon content of both the microcapsules and the PS particles is needed, being 41.77 %wt and 49.79 %wt respectively.

Table 3.1 Coatings developed and their principal characteristics

	coating material	particles	particles concentration (g/l)	current density (A/dm^2)	temperature (ºC)	sample thickness (µm)	carbon content (%wt)	particles (%vol)
Cuµcap100	copper	microcapsules	100	2	25	100	0.8608	8.15
Cuµcap200	copper	microcapsules	200	2	25	100	1.5978	15.26
Cuµcap300	copper	microcapsules	300	2	25	100	2.3814	22.93
CuPS100	copper	PS particles	100	2	25	100	0.9230	7.35
CuPS200	copper	PS particles	200	2	25	100	2.0479	16.46
CuPS300	copper	PS particles	300	2	25	100	2.2207	17.93
Cu pure	copper	none	0	2	25	100	0	0
Niµcap100	nickel	microcapsules	100	2	55	100	0.5815	5.5
Niµcap200	nickel	microcapsules	200	2	55	100	0.7559	7.16
Niµcap300	nickel	microcapsules	300	2	55	100	0.9488	9.02
NiPS200	nickel	PS particles	200	2	55	100	0.8213	6.54
NiPS300	nickel	PS particles	300	2	55	100	1.0937	8.72
Ni pure	nickel	none	0	5	55	100	0	0

3.2.1 Preparation of the electrolytes

The copper and nickel coatings were developed by electrodeposition of PS particles and microcapsules in order to study their properties, focusing on their thermal expansive behaviour.

The microcapsules and solid polystyrene particles were added in three different concentrations: 100 g/l, 200 g/l and 300 g/l.

3.2.2 Samples pre-treatment

Before doing each electrodeposition, the substrates, consisting in aluminium cylinders, must be pre-treated for obtaining the appropriate coatings.

The pre-treatments done to aluminium cylinders consisted in:

- grounding with grinding paper making edges parallel and improving coatings´ adherence
- degreasing with acetone, wiping with paper and then rinsing with water
- painting with electrically isolating Nolan lacquer such that each active part of height 1 cm remains
- degreasing in an alkaline solution with a concentration of 50 g/l at 80 °C during 1 minute
- rinsing with water
- washing in a water solution with 10 %vol H_2SO_4
- rinsing with water

A PFTE stirrer was mounted at the end of the rotating cylinder cathode for enhancing the agitation of the bath.

3.2.3 Electrodeposition of copper coatings

The acidic copper sulphate electrolyte consisted in 200 g/l of $CuSO_4.5H_2O$ and 100 g/l H_2SO_4.

Copper coatings were made at room temperature, at a rotating speed of 300 rpm and at a current density of 2 A/dm^2.

The duration of the electrodeposition depends on the desired thickness. In this case, coatings were 100 μm thick. The standard coating growth value for copper II is 0.221 μm/min with a current density of 1 A/dm^2. In our case, it was 0.442 μm/min as a current density of 2 A/dm^2 was applied.

To calculate times spent in the development of the coatings, Faraday equations were applied:

$$S_{Al\_cylinder} = \pi Dh = \pi 4.6 \cdot 10^{-3} \cdot 10^{-2} = 1.445 \cdot 10^{-4} m^2 = 1.445 \cdot 10^{-2} dm^2 \quad (3.1)$$

$$2A/dm^2 = \frac{I}{S} = \frac{I}{1.445 \cdot 10^{-2}} \longrightarrow I = 28.9mA \quad (3.2)$$

$$t_{100\mu m} = \frac{100\mu m}{0.442\mu m/\min} = 226.24\min \cong 3h46\min \quad (3.3)$$

3.2.4 Electrodeposition of nickel coatings

Initially, a Watts bath containing 300 g/l of $NiSO_4 \cdot 6H_2O$, 40 g/l of $NiCl_2 \cdot 6H_2O$ and 40 g/l of H_3BO_3 plus $2 \cdot 10^{-4}$ M of CTAHS surfactant (cetyltrimethyl ammonium hydrogensulfate) was used. The mission of the surfactant is to reduce the incorporation of hydrogen gas bubbles in the coating and to avoid its consequent embrittlement.
However, the high stresses in the coatings obtained using the Watts bath provoked that they were not as satisfactory as expected because of their flaky finish.

Instead of the mentioned Watts bath, another nickel bath composed by 1M of $Ni(NH_2SO_3)_2 \cdot 4H_2O$ and 30 g/l of H_3BO_3 and pH of 3 was finally used. The results were then widely more adequate, with a good surface quality, uniformity, without scales and no embrittlement because of the hydrogen entrapment although no surfactant was added to the bath.

Figure 3.9 Rotating machine, current source and thermostatic bath

The nickel coatings were made at 55 ºC by using a double walled beaker and a thermostatic bath at a rotating speed of 300 rpm and at a current density of 2 A/dm^2, except in the case of the pure nickel coating which was done at 5 A/dm^2.

The time of electrodeposition depends on the desired thickness, in this case 100 μm. The standard coating growth value for nickel II is 0.205 μm/min with a current density of 1 A/dm^2. For particles coatings, it was 0.410 μm/min as 2 A/dm^2 was applied and 1.025 μm/min as 5 A/dm^2 was applied for pure nickel coatings.

To calculate times needed in the experiments, Faraday equations were again applied:

$$S_{Al\_cylinder} = \pi Dh = \pi 4.6 \cdot 10^{-3} \cdot 10^{-2} = 1.445 \cdot 10^{-4} m^2 = 1.445 \cdot 10^{-2} dm^2 \quad (3.4)$$

Pure nickel coating: $5A/dm^2 = \frac{I}{S} = \frac{I}{1.445 \cdot 10^{-2}} \longrightarrow I = 72.3mA$ (3.5)

$$t_{100\mu m} = \frac{100\mu m}{1.025\mu m/\min} = 97.56\min \cong 1h38\min \quad (3.6)$$

Nickel with particles coating: $2A/dm^2 = \frac{I}{S} = \frac{I}{1.445 \cdot 10^{-2}} \longrightarrow I = 28.9mA$ (3.7)

$$t_{100\mu m} = \frac{100\mu m}{0.410\mu m/\min} = 243.9\min \cong 4h4\min \quad (3.8)$$

3.2.5 Samples post-treatment

Once the coatings had been obtained, the extremes of the samples were grinded in order to make them completely parallel for using them in the subsequent tests of thermal dilatometry.

After that, aluminium substrates were dissolved by submerging cylinders in a solution 2M of KOH in water at 75 ºC contained in a nickel recipient to avoid possible degradation in case of using a recipient made of glass. After that, the resultant samples are rinsed first in water, then in ethanol; subsequently, they are dried.

3.2.6 Samples cross section micrographs

In order to observe the samples cross section before and after the thermal dilatometry in the optical microscope, they were mounted using fast resin and grinded until the surface was completely smooth without scratches.

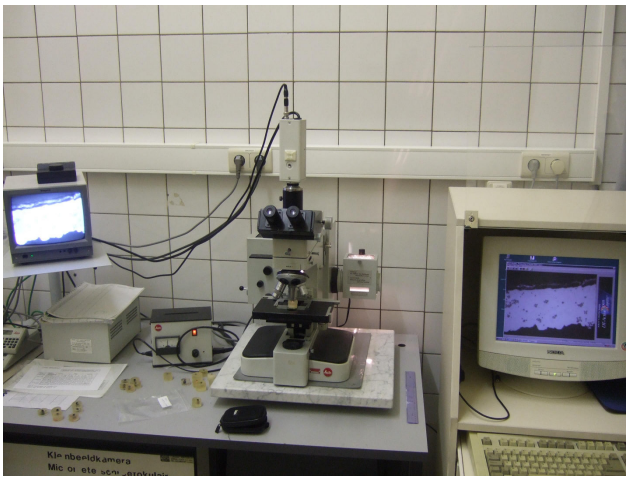

Figure 3.10 Optical microscope

The magnification used in all the samples is 32x and their thickness is indicated in each picture. Pictures after thermal dilatometry will be shown in next chapter.

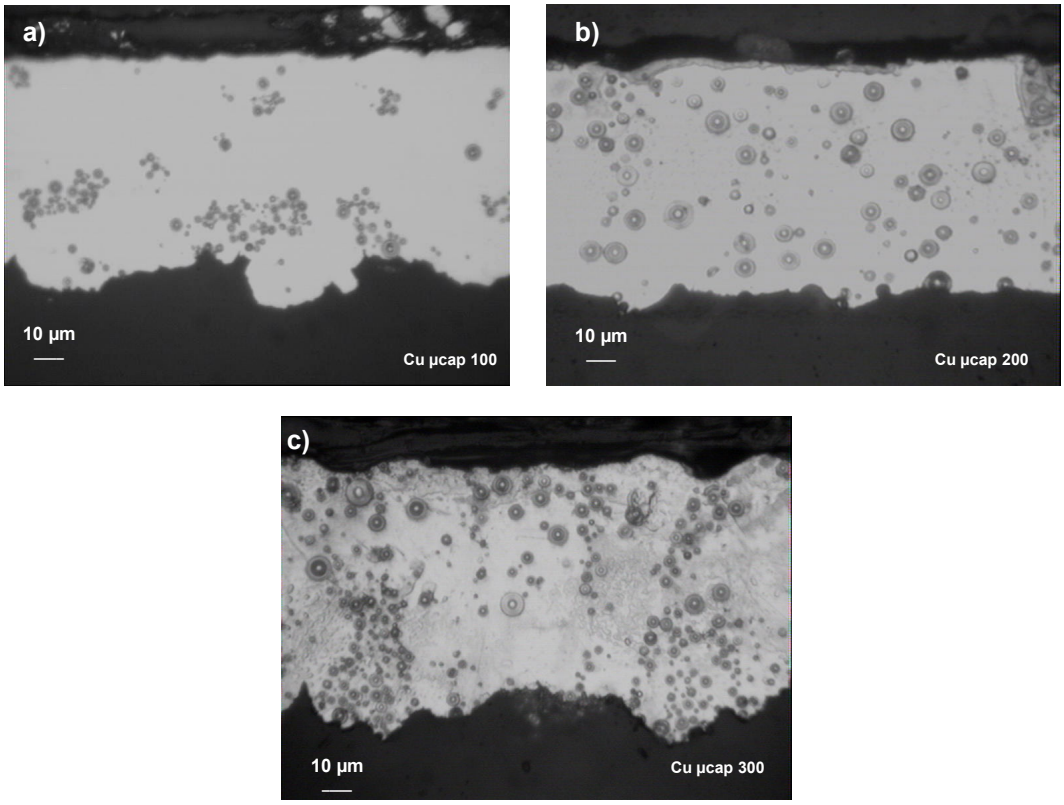

Figure 3.11 Copper coatings containing 100 g/l (a), 200 g/l (b) and 300 g/l (c) of microcapsules respectively

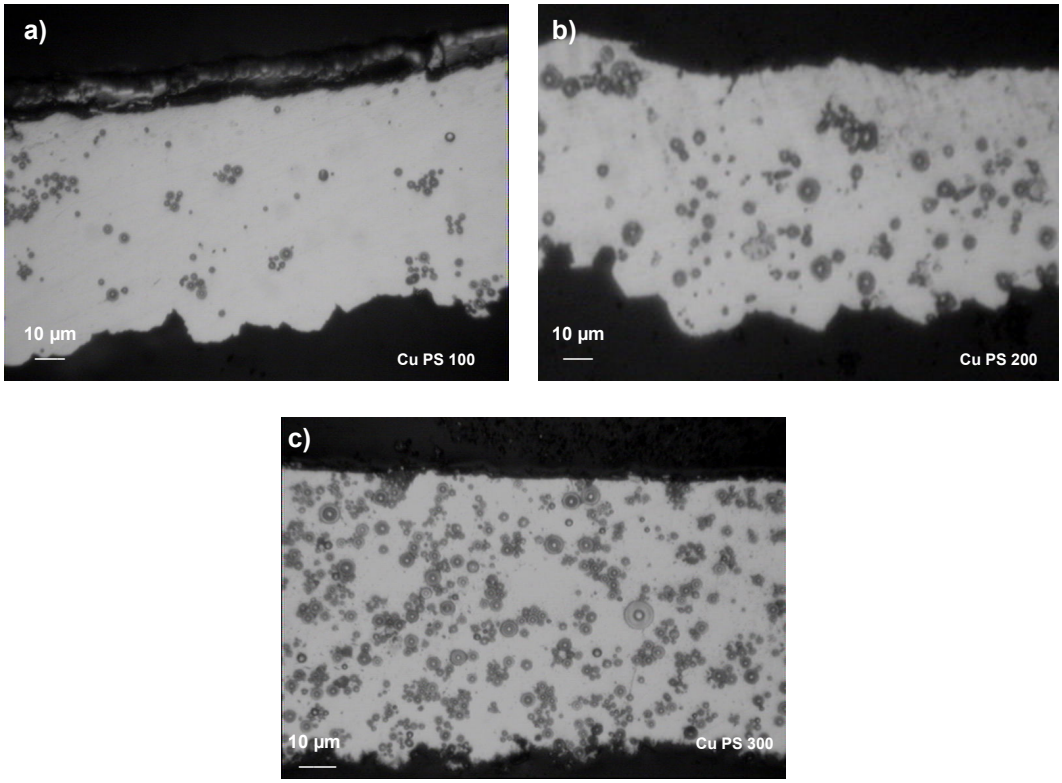

Figure 3.12 Copper coatings containing 100 g/l (a), 200 g/l (b) and 300 g/l (c) of PS particles respectively

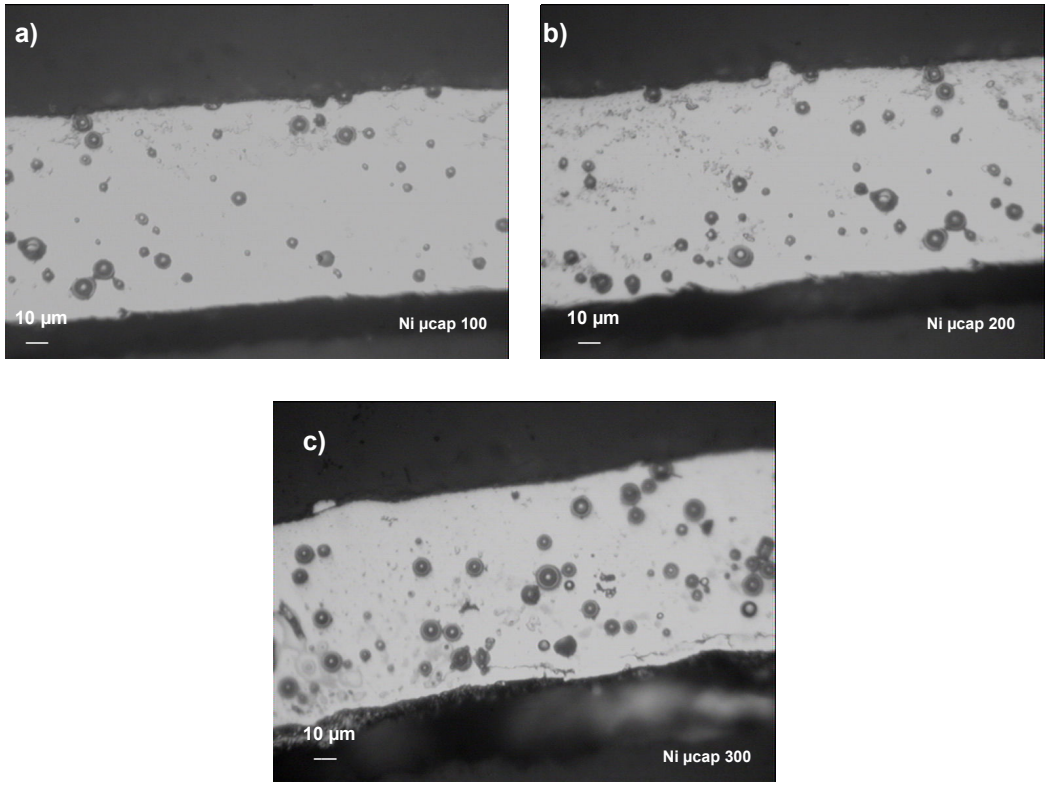

Figure 3.13 Nickel coatings containing 100 g/l (a), 200 g/l (b) and 300 g/l (c) of microcapsules respectively

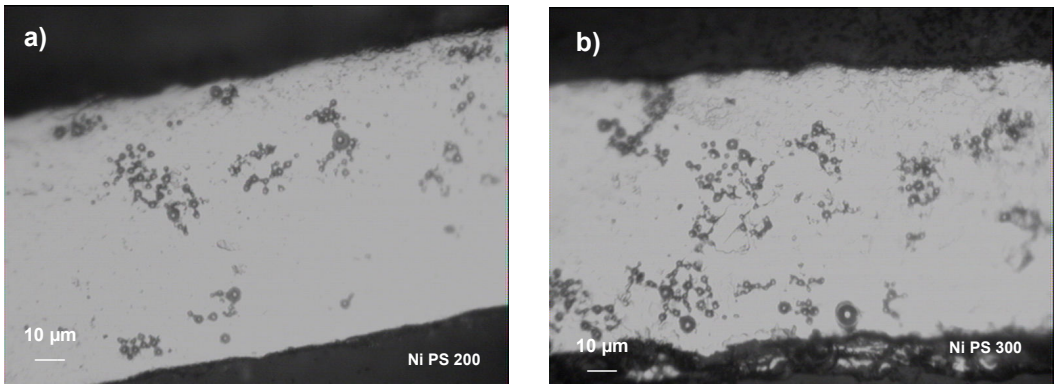

Figure 3.14 Nickel coatings containing 100 g/l (a) and 200 g/l (b) of PS particles

Chapter 4: *Samples testing and results analysis*

4.1 Differential scanning calorimetry (DSC)

The heat flow during the phase transformation of the particles embedded in the metal matrix is measured by using differential scanning calorimetry (DSC). The measures are performed in a Q2000 Modulated DSC from TA Instruments.

Figure 4.1 Differential scanning dilatometer Q2000 from TA Instruments

The differential scanning calorimetry can be:

- Static: the samples are heated until reaching a selected temperature, which is maintained during the test. The output is the heat flux as a function of the time.
- Dynamic: the samples are heated with a constant heating rate until reaching a selected temperature. The output is the heat flux as a function of the temperature.

The samples and the reference pure metal are placed in closed aluminium containers with helium as inert atmosphere.

The heating and cooling rate applied during experiments is 10 ºC/min from room temperature until 550 ºC is reached in the first cycle and from 40 ºC to 550 ºC during both the second and third cycles. The extreme temperatures (40 ºC and 550 ºC) are maintained for 3 minutes.

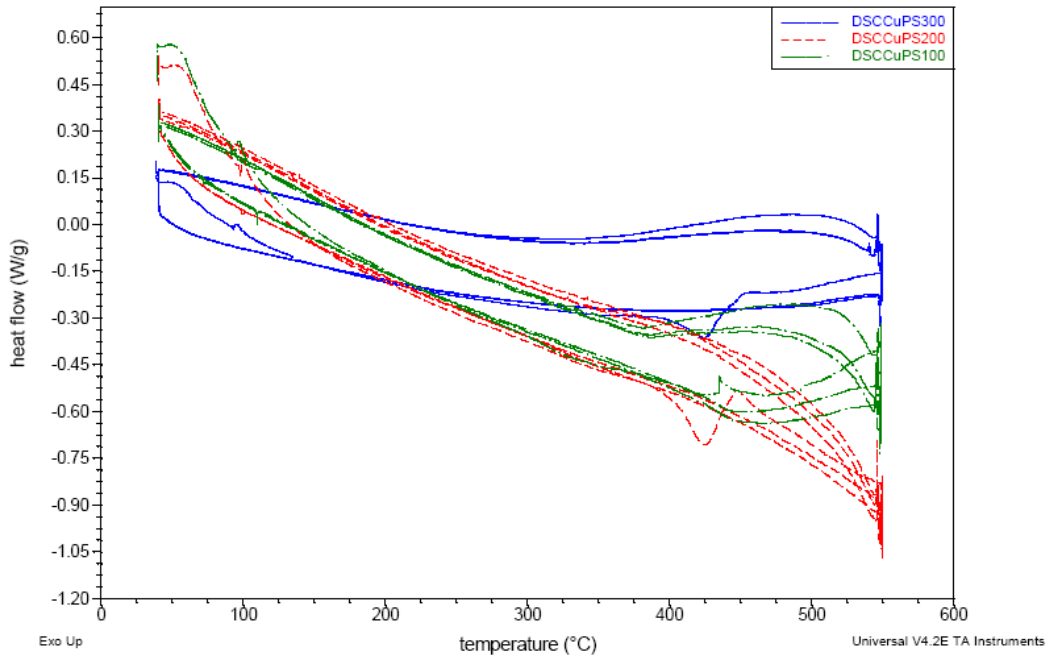

Figure 4.2 Full DSC test for copper coatings containing 300 g/l (17.93 %vol), 200 g/l (16.46 %vol) and 100 g/l (7.35 %vol) of PS particles. Heating rate: 10 ºC/min from 40 ºC to 550 ºC maintaining the extreme temperatures (40 and 550ºC) during 3 minutes. Helium atmosphere

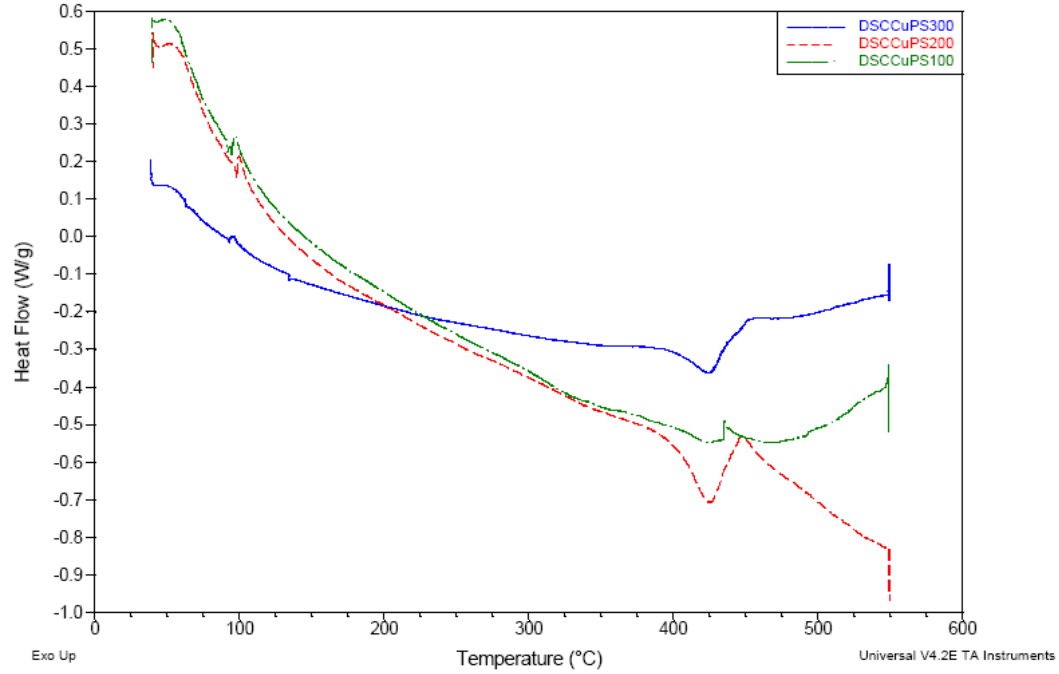

Figure 4.3 Comparative of the first DSC cycle of copper coatings containing PS particles

When analysing the first heating cycle of the DSC curves of copper coatings containing PS particles several peaks are detected and related with changes in the structure of the polystyrene (Figure 4.3).

At 100 ºC appears a small endothermic peak because of the glass transition temperature of the PS. In standard conditions this value would be below 90 ºC. However, the obtained one is higher because of the pressure increment over the particles exerted by the metal

matrix due to the heating. This pressure rise will displace all the temperatures of the structural changes to higher values.
From this temperature until reaching the degrading temperature at 425 ºC, the curves show a lightly endothermic process due to the polymer chains reorganization.
At 400 ºC, the PS particles start their degradation in an endothermic process. It coincides with the theoretical value for standard conditions, where the pure PS degrades at 398.77 ºC for a heating rate of 10 ºC/min. This coincidence is caused by the softening of pure copper at temperatures around 400 ºC accompanied by an increase in its thermal expansion coefficient which allows PS particles expanding during the degradation process.

The degradation reactions involved in PS include random scission (which reduces the molecular weight of the polymer), de-polymerization (which yields monomer), intra-molecular transfer reaction (which produces dimer, trimer, etc.) and intermolecular transfer reaction which reduces the molecular weight of the polymer; all these degradation reactions may produce short-chain polymer fragments if they take place near the chain end, and they have the effect of increasing the number of active centres.[8]

The products obtained after the degradation are mainly styrene monomer, benzene, toluene, light hydrocarbons, some dimers (2,4–diphenyl–1–butane) and trimers (2,4,6–triphenyl–1–hexane) as volatile products and a residue above 430 ºC which may consist of some condensed products.

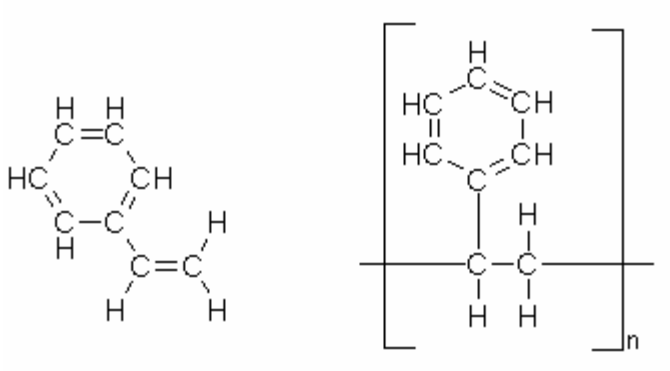

Figure 4.4 Styrene and polystyrene structures

The thermal decomposition temperature for PS increases with higher heating rates due to the lower exposure to heat as the degradation time has been reduced if the heating rates are higher. At low heating rates presence of some cross-linked products is evident at temperature around 400 – 500 ºC whereas at higher heating rates the volatile products may not get sufficient time in the matrix to condense with each other. During thermal dilatometry tests, the heating rate is 3 ºC/min, which will lead into a thermal degradation temperature for polystyrene around 360 ºC. [9]

As a result, copper coatings containing PS particles suffer the highest expansion from 360 ºC on. In the case of nickel coatings, the expansion increment is delayed until 400 ºC because of the higher elastic modulus of nickel (207 GPa) compared to copper (115 GPa) and its lower content in volume fraction of particles (figures 4.11 and 4.19).

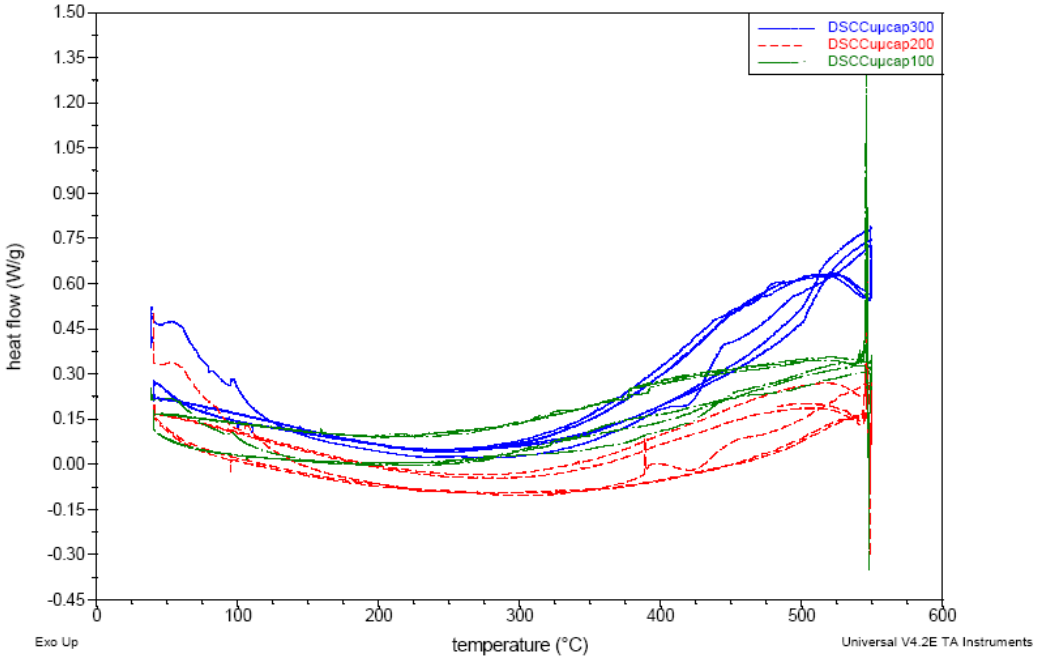

Figure 4.5 Full DSC test for copper coatings containing 300 g/l (22.93 %vol), 200 g/l (15.26 %vol) and 100 g/l (8.15 %vol) of microcapsules. Heating rate: 10 ºC/min from 40 ºC to 550 ºC maintaining the extreme temperatures (40 and 550ºC) during 3 minutes. Helium atmosphere

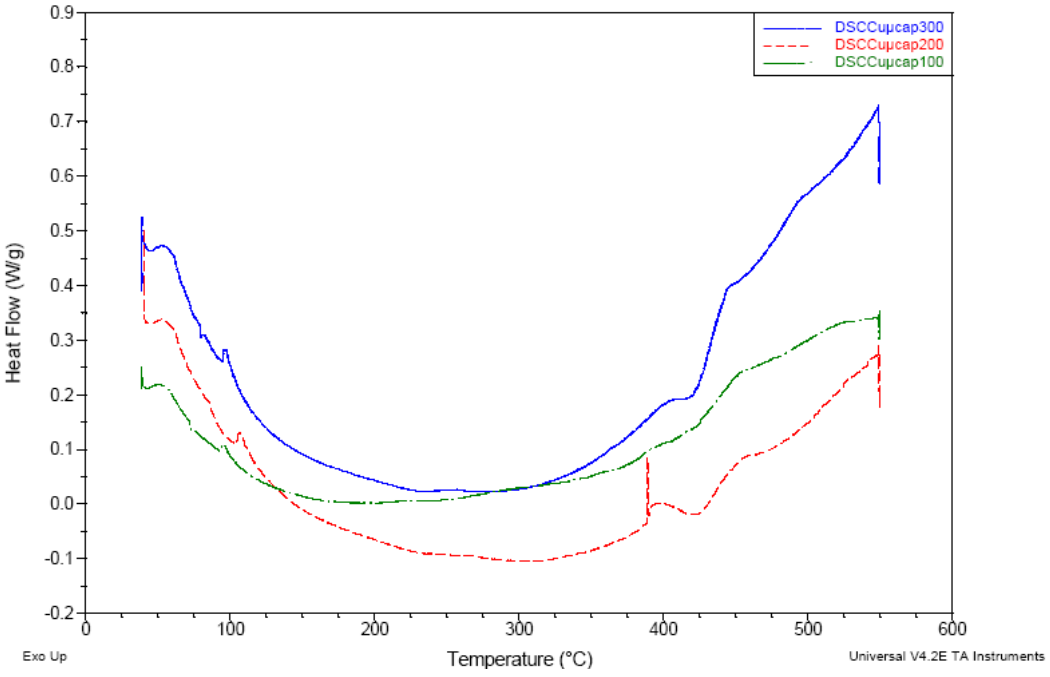

Figure 4.6 Comparative of the first DSC cycle of copper coatings containing microcapsules

In the case of the copper coatings containing microcapsules, the water contained inside them has a boiling trajectory instead a boiling point at 100 ºC. However, a small exothermic peak can be noticed at 100 ºC due to the water boiling start or maybe because of the glass transition temperature of the polymer shell of the microcapsules.

In the DSC curves can be seen how water is evaporated in subsequent volume fractions from 200 ºC to 400 ºC approximately because the curve is almost plane as thermal energy is employed in changing water phase from liquid to gas. That effect is caused by

having a boiling trajectory instead of a boiling point. After the evaporation, the process starts being exothermic.

As a result, copper and nickel coatings containing microcapsules experiments the highest expansion from 375 ºC on (figures 4.11 and 4.19).

4.2 Thermal dilatometry (TD)

The thermal dilatometry shows the dimension changes of samples when heat is applied at different rates. The expansion or contraction is measured in one direction using a feeler in constant contact with the sample during the running test applying a small force on it, in this case 0.05N.

Figure 4.7 Horizontal thermal dilatometer

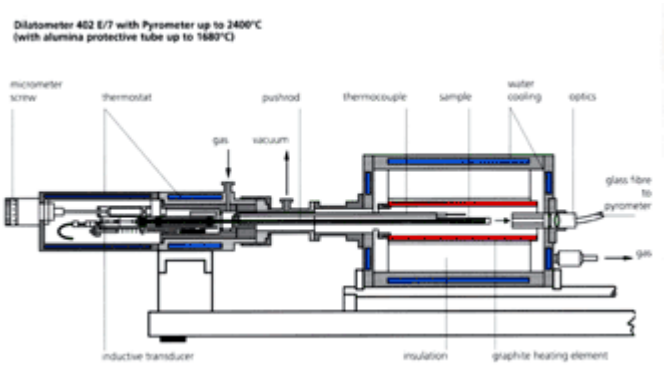

Figure 4.8 Thermal dilatometer scheme

In order to measure the thermal expansion of our samples, a vertical dilatometer TMA Q400 from TA Instruments was used. The force applied on the samples was 0.05 N.

Figure 4.9 Thermal dilatometer TMA Q400 from TA Instruments

Two different thermal dilatometry tests were performed with full or partial heating cycles.

The first test consisted in the application of three full heating cycles: from room temperature to 600 ºC in the first one, and then from 50 ºC to 600 ºC in both the second and the third cycles.

The second test consisted in the application of three partial heating cycles: from room temperature to 200ºC in the first one, from 50 ºC temperature to 400 ºC in the second one and from 50 ºC to 600 ºC in the third one.

In both cases, the temperature reached at the end of each cycle (600, 400, 200, 50 ºC or room temperature in each case) is maintained for 2 minutes. The heating rate applied is 3 ºC/min and argon is used as inert atmosphere.

The results are displayed in two different types of graphs.

- The first type is made by using the analysis program Universal analysis 2000 of TA Instruments where expansion in µm is represented versus temperature in ºC. These results are not completely veridical as samples have different initial lengths and therefore the expansion obtained changes depending on them.
- The second type of graphs is made by using the program Excel of Microsoft. In this case, expansion in percentage is represented versus temperature in ºC. These results are more reliable and not dependant on the initial length of the samples.

It must be taken into account that some results are not displayed because samples were broken while performing the tests.

4.2.1 Thermal dilatometry results and analysis

4.2.1.1 Copper coatings

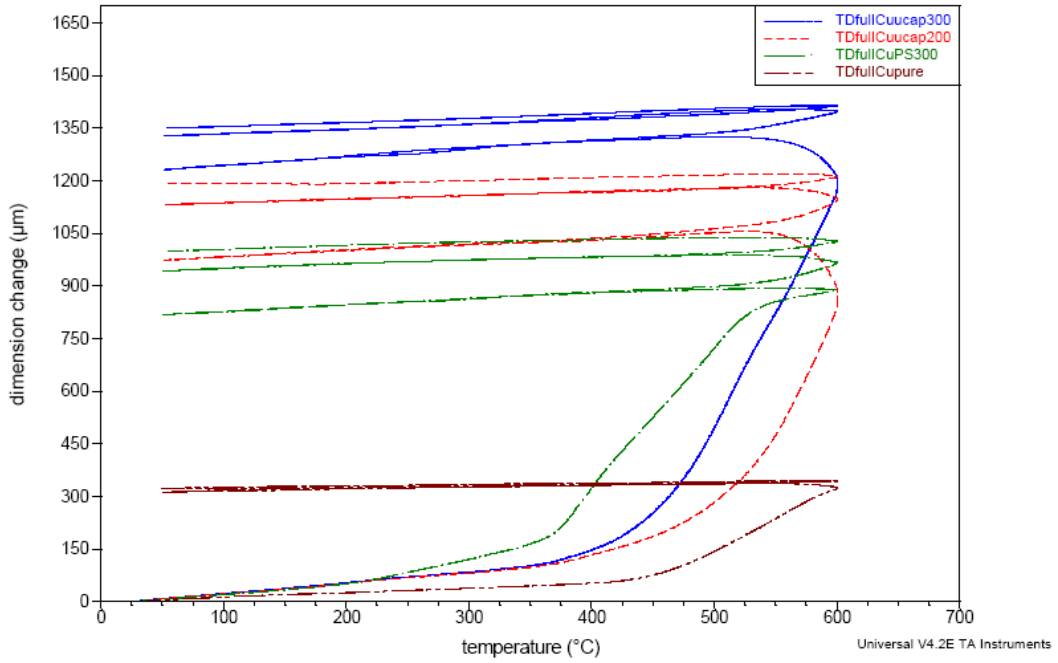

Figure 4.10 Full cycle thermal dilatometry of copper coatings containing 300 g/l (22.93 %vol) and 200 g/l (15.26 %vol) of microcapsules and 300 g/l (17.93 %vol) of PS particles compared with pure copper. Characteristics: Heating rate: 3 ºC/min from room temperature to 600 ºC in the first cycle and from 50 ºC to 600 ºC in both the second and third cycles maintaining both extreme temperatures (50 and 600 ºC) during 2 minutes (isothermal). Argon atmosphere. Initial lengths: Cuucap300 (16.3197 mm), Cuucap200 (15.3757 mm), CuPS300 (14.0943) and pure Cu (12.42 mm)

During the first heating cycle of copper samples, it is noticed a quasi-linear expansion behaviour of the coatings containing microcapsules and the pure copper sample until 375 ºC with mainly elastic deformation and little plastic deformation. At higher temperatures, the deformation is mainly plastic, with a sharp increment in the slopes of the curves. In the case of pure copper it is caused by its recrystallisation, which occurs at around 425 ºC.

In the case of coatings containing PS particles, the plastic deformation starts smoothly at 200 ºC, due to the higher thermal expansion coefficient of PS compared to the water's value. At 375 ºC, a sharp increment in plastic deformation is produced.

During the second cycle, the deformation is still predominately plastic and passes the 1 % as can be observed in figure 4.12.

Comparing figure 4.10 with figure 4.11, it is noticed the non correspondence between measured expansion in µm and expansion in percentage as said before.

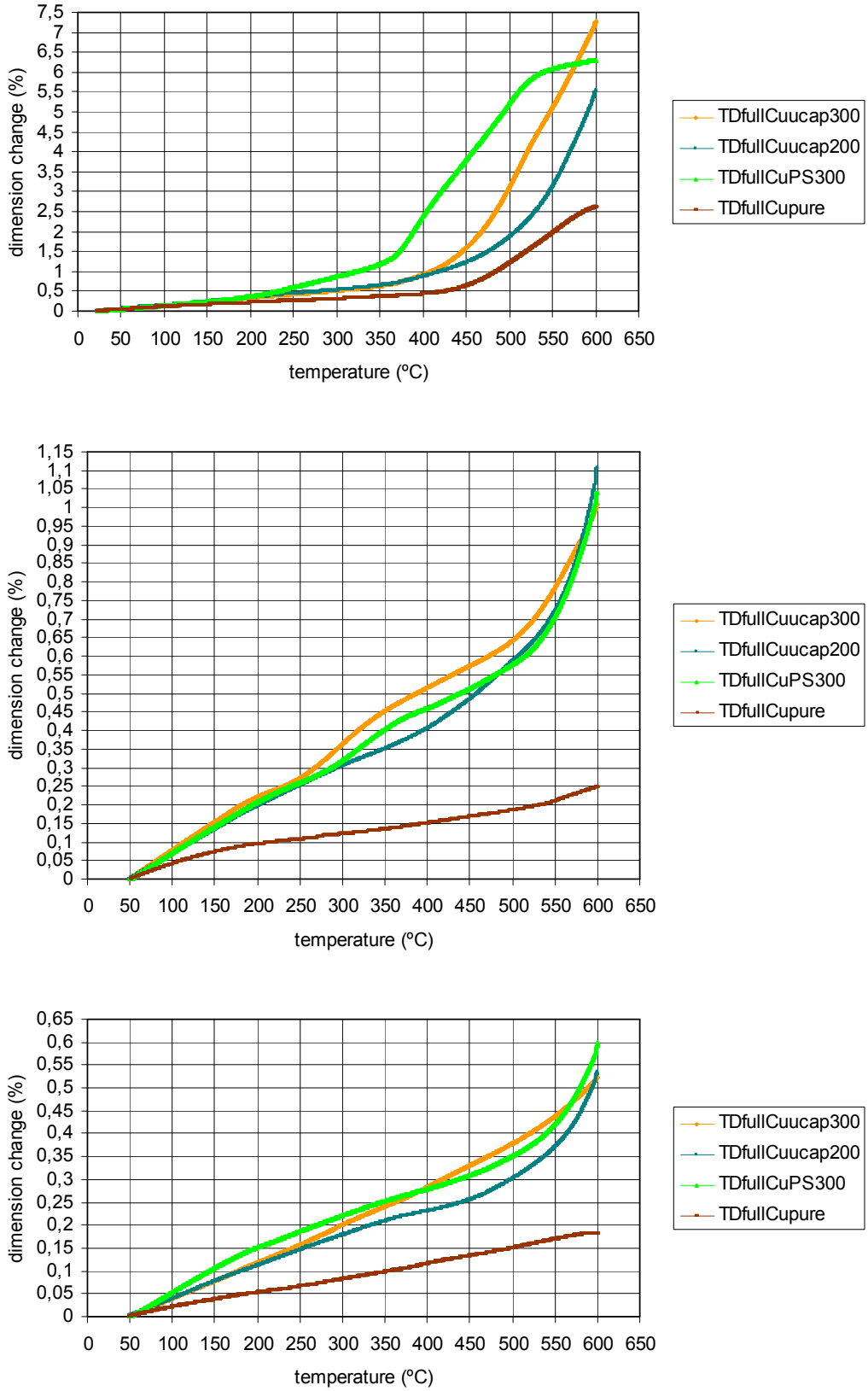

Figures 4.11, 4.12, 4.13 Comparative of the dimension change in percentage during the first, second and third full heating cycle between copper coatings containing 300 g/l (22.93 %vol) and 200 g/l (15.26 %vol) of microcapsules, 300 g/l (17.93 %vol) of solid polystyrene particles and pure copper

In the case of full cycling of copper samples, the expansion behaviour depends on which cycle is running because of the plastic deformation suffered by the matrix during the first cycle. As a consequence, during second and third cycles, both the microcapsules and the PS particles can expand causing little or even without plastic deformation.

In the first heating cycle (figure 4.11) all the samples show several slopes in different temperatures ranges. These slopes are related to the thermal expansion coefficient by the equation:

$$\frac{\Delta l}{l_0} = \alpha \Delta T \longrightarrow \alpha = \frac{\Delta l}{l_0 \cdot \Delta T} \tag{4.1}$$

In Table 4.1 the different thermal expansion coefficients are shown at different temperature ranges. The measurements have been taken in small temperature ranges (25 ºC) in order to find the adequate working range of each sample for being used as a thermo actuator.

Table 4.1 Thermal expansion coefficients of copper samples at different temperatures ranges

	thermal expansion coefficient α ($ºC^{-1} \cdot 10^{-6}$)			
temperature range (ºC)	**Cuucap300 (22.93%vol)**	**Cuucap200 (15.26%vol)**	**CuPS300 (17.93 %vol)**	**pure Cu**
25-50	18.19	17.85	17.35	13.06
50-75	19.30	18.97	18.36	12.36
75-100	17.25	17.54	18.26	13.65
100-125	18.06	17.76	19.16	13.19
125-150	16.81	16.04	19.92	9.52
150-175	19.60	20.03	21.79	7.77
175-200	20.65	21.95	19.08	9.06
200-225	20.71	24.02	38.36	10.41
225-250	18.87	20.18	53.45	10.14
250-275	16.67	15.64	51.94	8.69
275-300	18.07	18.31	53.93	9.90
300-325	20.24	20.56	57.25	10.98
325-350	24.09	22.05	66.84	11.40
350-375	41.48	32.56	137.39	13.00
375-400	68.21	55.95	321.19	13.18
400-425	97.97	62.20	300.63	23.78
425-450	159.73	73.44	270.50	53.21
450-475	236.04	100.88	272.93	91.37
475-500	350.25	145.05	285.97	129.83
500-525	425.01	196.23	254.34	146.47
525-550	377.29	284.14	116.43	154.74
550-575	397.77	418.76	49.92	155.62
575-600	508.99	514.22	44.51	122.19

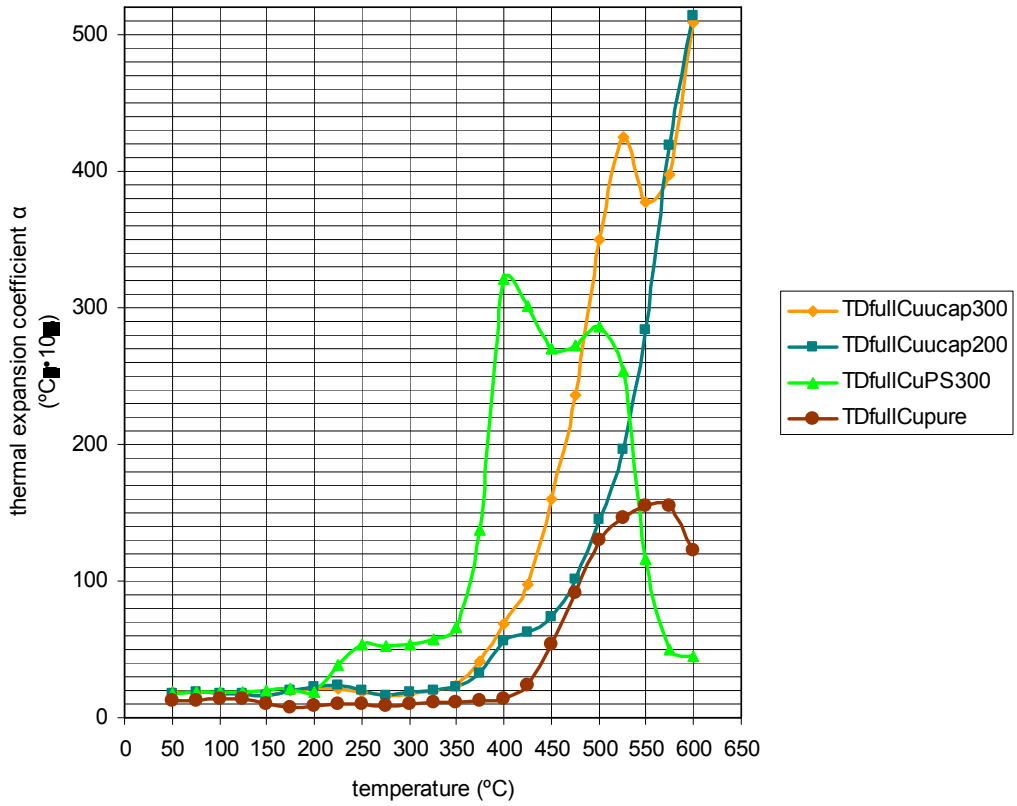

Figure 4.14 Variation of the thermal expansion coefficients of copper samples with temperature

While studying the thermal expansion coefficients change with temperature in order to analyse their potential applicability as thermo actuators, several conclusions can be found if Table 4.1 and Figure 4.14 are observed.

In the case of copper coatings containing 300 g/l (22.93 %vol) of microcapsules, a sharp increment is observed in the temperature range from 350 ºC to 525 ºC (α = 383.53·10^{-6} ºC^{-1}) and from 550 ºC to 600 ºC (α = 131.7·10^{-6} ºC^{-1}). In the sample containing 200 g/l (15.26 %vol), the sharp increment goes from 350 ºC to 600 ºC (α = 481.66·10^{-6} ºC^{-1}). These results make that coatings containing microcapsules become effective thermo actuators.

For low temperatures range (below 200 ºC), all the samples behave in a quasi-linear way. Samples containing particles have almost the same slope (around 20·10^{-6}) and it approximately doubles the pure copper's one (10·10^{-6}).

In the case of copper containing 300 g/l (17.93 %vol) of PS particles, there are several increments and decrements in the thermal expansion coefficient at different temperatures ranges: from 200 ºC to 250 ºC (α = 34.37·10^{-6} ºC^{-1}), from 350 to 400 ºC (α = 254.35·10^{-6} ºC^{-1}), from 400 ºC to 450 ºC (α = -50.69·10^{-6} ºC^{-1}) and from 500 ºC to 575 ºC (α = -236.05·10^{-6} ºC^{-1}).
These negative values can be explained by a possible condensation of the gases produced during the degradation of PS because of the high pressure reached inside the coating.

Pure copper also experiments a sharp increment in its thermal expansion coefficient in the temperature range from 425 ºC to 500 ºC (α = 122.69·10^{-6} ºC^{-1}).

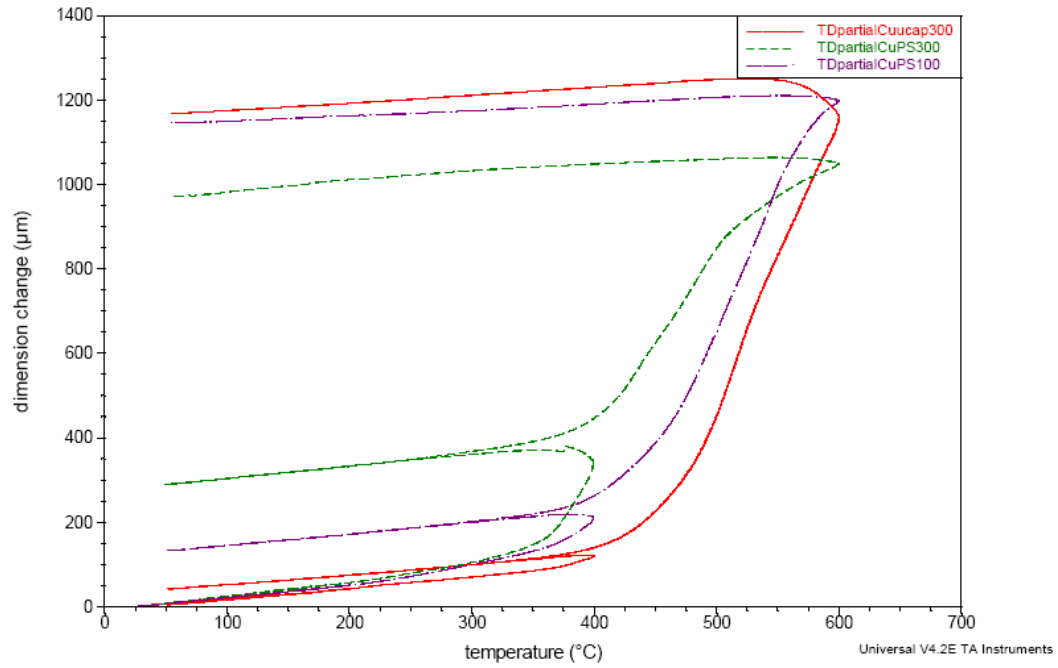

Figure 4.15 Partial cycle thermal dilatometry of copper coatings containing 300 g/l (22.93 %vol) of microcapsules and 300 g/l (17.93 %vol) and 100 g/l (7.35 %vol) of PS particles. Characteristics: Heating rate: 3 ºC/min from room temperature to 200 ºC in the first cycle, from 50 ºC to 400 ºC in the second cycle and from 50 to 600 ºC the third cycle maintaining the extreme temperatures (50, 200, 400 and 600 ºC) during 2 minutes (isothermal). Argon atmosphere. Initial lengths: Cuucap300 (13.7090 mm), CuPS300 (17.6699 mm), CuPS100 (16.1475 mm)

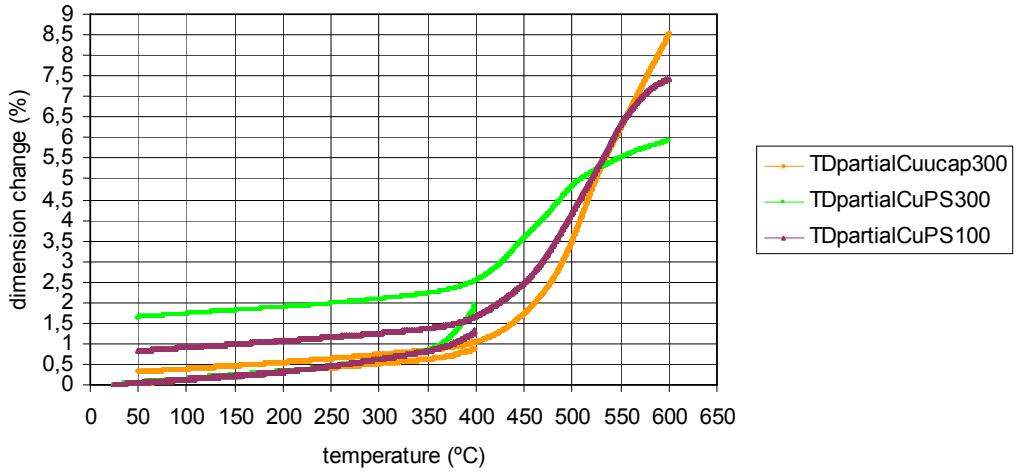

Figure 4.16 Comparative of the dimension change in percentage during the partial heating cycles from room temperature to 200 ºC, 50-400 ºC and 50-600 ºC between copper coatings containing 3 00 g/l (22.93 %vol) of microcapsules and 300 g/l (17.93 %vol) and 100 g/l (7.35 %vol) of PS particles

In the case of partial cycling of copper samples, the results are also dependent on the studied cycle (Figures 4.15 and 4.16).

For the first cycle, from room temperature to 200 ºC, all the samples have the same behaviour as the PS particles and microcapsules remain intact without boiling or degradation. The whole expansion produced is elastic as the samples recover their original shape after the thermal load.

During the second cycle, from 50 ºC to 400 ºC, the coatings containing PS particles start to suffer plastic deformation that remains during subsequent cycles without any recovery. The highest expansion values were obtained in the sample containing 300 g/l of PS particles, with quasi-linear behaviour until 350 ºC and a sharp expansion increment starting at that temperature because of the PS degradation. The sample containing 100 g/l of PS particles expands in a similar way until 350 ºC and then it has a smooth increment because of the lower content in particles. In the meanwhile, the coating with 300 g/l of microcapsules has quasi-linear expansion behaviour until 375 ºC and from that point on it starts to expand slowly. However, it expands both elastically and plastically as it recovers part of its deformation during cooling.

In the third cycle, from 50 to 600 ºC, the samples with PS particles maintain the deformation reached in the previous cycle whereas the sample with microcapsules recovers part of this deformation. The CuPS300 sample experiments the highest expansion, followed by the CuPS100 one, until the temperature 525 ºC is reached. From 525 ºC to 600 ºC, the results were opposite, the sample Cuucap300 expands linearly until it reached 8.5 %, whereas CuPS100 reached 7.5 % and CuPS300 only 6 %. These values can be explained by a possible condensation the gases produced during the degradation of PS because of the high pressure reached inside the coating.

4.2.1.2 Nickel coatings

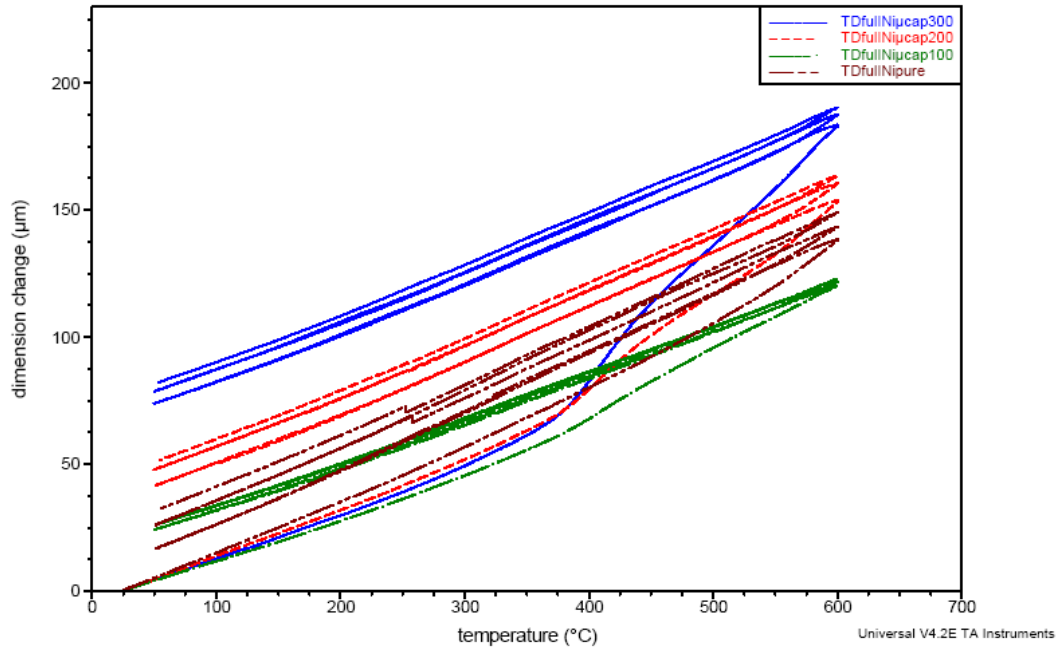

Figure 4.17 Full cycle thermal dilatometry of nickel coatings containing 300 g/l (9.02 %vol), 200 g/l (7.16 %vol) and 100 g/l (5.5 %vol) of microcapsules compared with pure nickel. Characteristics: Heating rate: 3 ºC/min from room temperature to 600 ºC in the first cycle and from 50 ºC to 600 ºC in both the second and third cycles maintaining both extreme temperatures (50 and 600 ºC) during 2 minutes (isothermal). Argon atmosphere. Initial lengths: Niucap300 (14.2568 mm), Niucap200 (13.6894 mm), Niucap100 (11.5005 mm) and pure Ni (14.7127 mm)

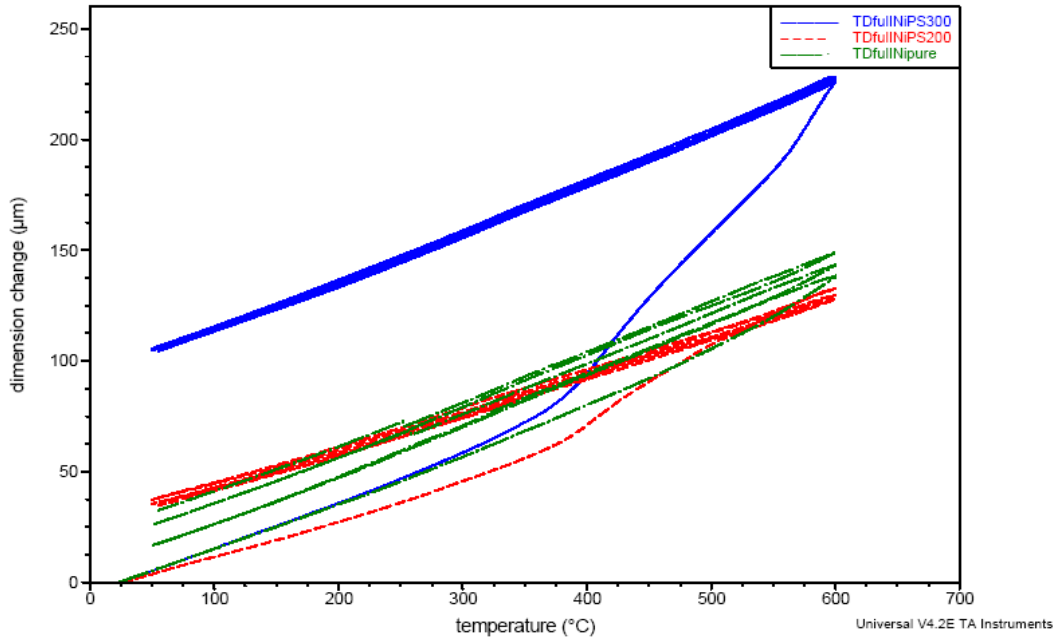

Figure 4.18 Full cycle thermal dilatometry of nickel coatings containing 300 g/l (8.72 %) and 200 g/l (6.54 %vol) of PS particles compared with pure nickel. Characteristics: Heating rate: 3 ºC/min from room temperature to 600 ºC in the first cycle and from 50 ºC to 600 ºC in both the second and third cycles maintaining both extreme temperatures (50 and 600 ºC) during 2 minutes (isothermal). Argon atmosphere. Initial lengths: NiPS300 (14.5978 mm), NiPS200 (11.2539 mm) and pure Ni (14.7127 mm)

In both Figures 4.17 and 4.18 can be seen how nickel samples recover a large part of the expansion occurred after heating (elastic). This effect happens thanks to the both higher elastic modulus and yield strength of nickel (207 GPa and138 MPa respectively) compared with those of copper (110 GPa and 69 MPa respectively). The elastic deformation occurs until reaching 375 ºC and it is detectable because of its linear behaviour (straight line) whereas the plastic one is defined by a change in slope with a curved line.

During second and third cycles, the expansion is completely elastic due to the big sized holes provoked by particles expansion after the first cycle.

These effects can be observed in Figures 4.19, 4.20 and 4.21, where elastic deformation is represented by straight lines as in the case of pure nickel, whereas plastic deformation appears as a sharp rise in the expansion value with a change in the slope.

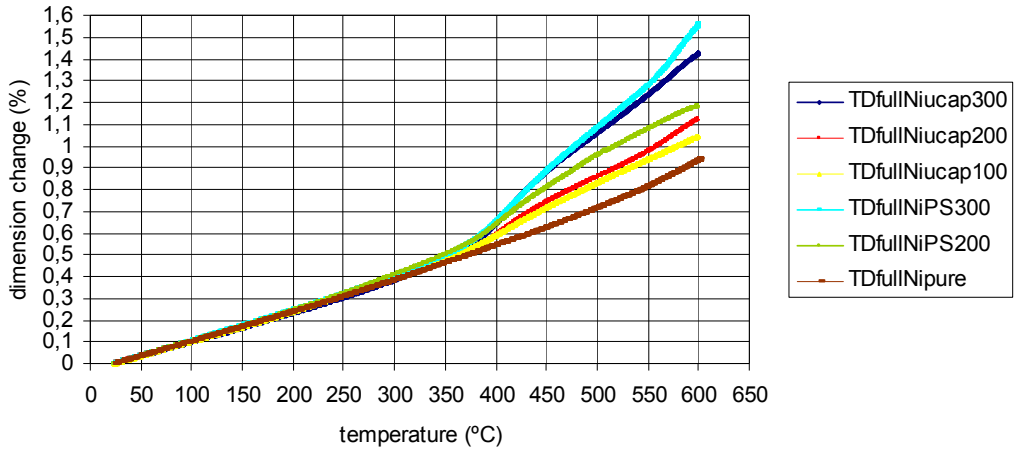

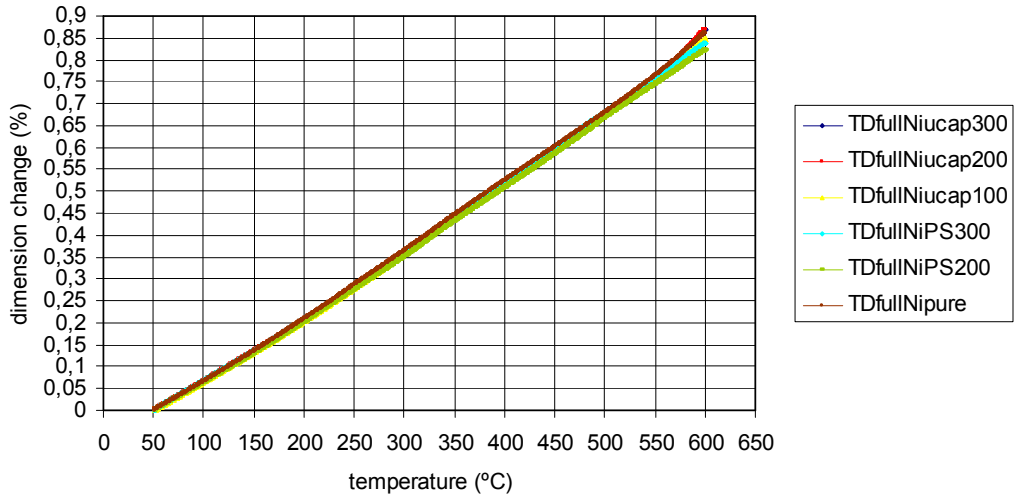

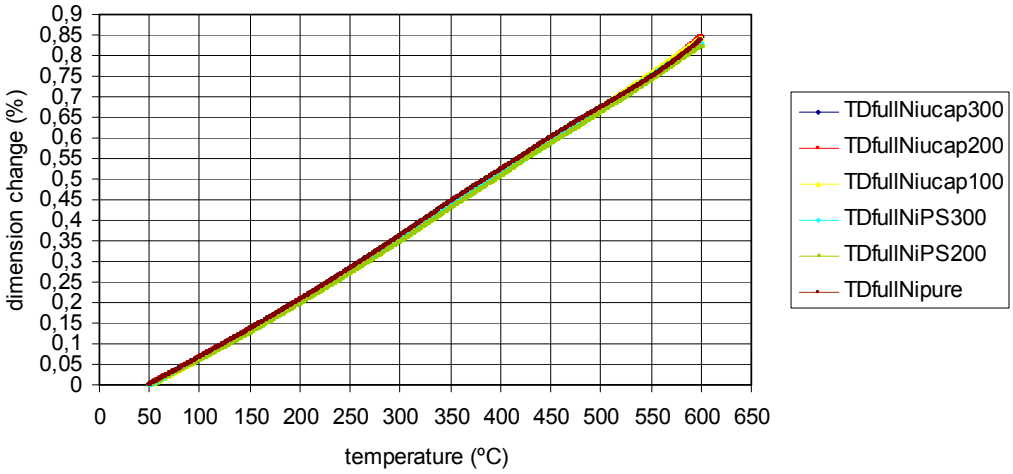

Figures 4.19, 4.20, 4.21 Comparative of the dimension change in percentage during the first, second and third full heating cycles between nickel coatings containing 300 g/l (9.02 %vol), 200 g/l (7.16 %vol) and 100 g/l (5.5 %vol) of microcapsules, 300 g/l (8.72 %vol) and 200 g/l (6.54 %vol) of PS particles and pure nickel

When analysing the thermal expansion behaviour of nickel coatings, all the samples behave in a similar way, with a quasi-linear expansion until 350 ºC is reached. The coatings having PS particles suffer a higher thermal expansion during the first heating cycle, even although their volume fraction of particles is lower. The coating of pure Ni does not suffer recrystallisation, as the temperature is not high enough.

Comparing the curves of Niucap300 (9.02 %vol particles) and NiPS300 (8.72 %vol particles), they behaves in a similar way until 450 ºC is reached. From that point on, the slope of curve NiPS300 has a sharper increment, and therefore its thermal expansion coefficient is higher. This is caused by the higher pressure exerted in the metal matrix by the gases produced during PS degradation compared with the one provoked by the vapour during microcapsules degradation.

In the case of Niucap200 (7.16 %vol particles) and NiPS200 (6.54 %vol particles), the mismatch starts just after 400 ºC.

During second and third cycles, the expansion suffered by the coatings containing particles is elastic and coincides with the pure nickel line.

The slopes of the different quasi-linear zones of each sample have been calculated because of their relationship with the thermal expansion coefficient.

Table 4.2 Thermal expansion coefficients of the nickel samples at different temperatures ranges

	thermal expansion coefficient α ($^oC^{-1}\cdot10^{-6}$)					
temperature range (ºC)	**Niucap300 (9.02%vol)**	**Niucap200 (7.16%vol)**	**Niucap100 (5.50%vol)**	**NiPS300 (8.72%vol)**	**NiPS200 (6.54%vol)**	**pure Ni**
25-50	12.99	12.73	12.78	12.89	13.25	12.48
50-75	12.44	13.63	13.71	13.81	14.23	13.57
75-100	13.05	13.49	13.14	13.88	13.23	13.41
100-125	12.59	13.04	13.35	13.95	13.21	13.54
125-150	13.38	12.77	13.10	13.72	13.66	13.34
150-175	13.79	13.50	13.98	14.23	14.46	13.93
175-200	13.28	13.36	14.51	14.24	14.77	13.77
200-225	14.01	13.67	14.74	14.71	15.10	13.64
225-250	14.74	14.75	15.36	15.40	15.84	14.45
250-275	15.61	14.76	16.04	15.95	16.71	15.23
275-300	16.41	15.23	16.13	16.60	18.24	15.20
300-325	18.42	16.08	17.00	17.90	17.67	15.65
325-350	19.14	17.28	18.16	19.77	19.25	15.91
350-375	24.28	19.53	18.76	23.90	21.87	15.78
375-400	42.27	29.45	23.69	37.43	32.21	16.46
400-425	52.05	33.49	26.57	48.66	37.30	16.08
425-450	42.99	27.80	24.53	45.10	32.11	16.67
450-475	36.98	24.08	23.01	40.66	29.30	17.51
475-500	34.43	22.39	22.92	38.92	29.93	18.56
500-525	34.36	22.11	21.79	37.94	23.67	19.11
525-550	35.74	24.69	21.05	39.52	24.45	20.57
550-575	38.91	29.26	21.26	51.92	23.38	23.86
575-600	38.39	30.32	21.75	61.96	17.78	25.18

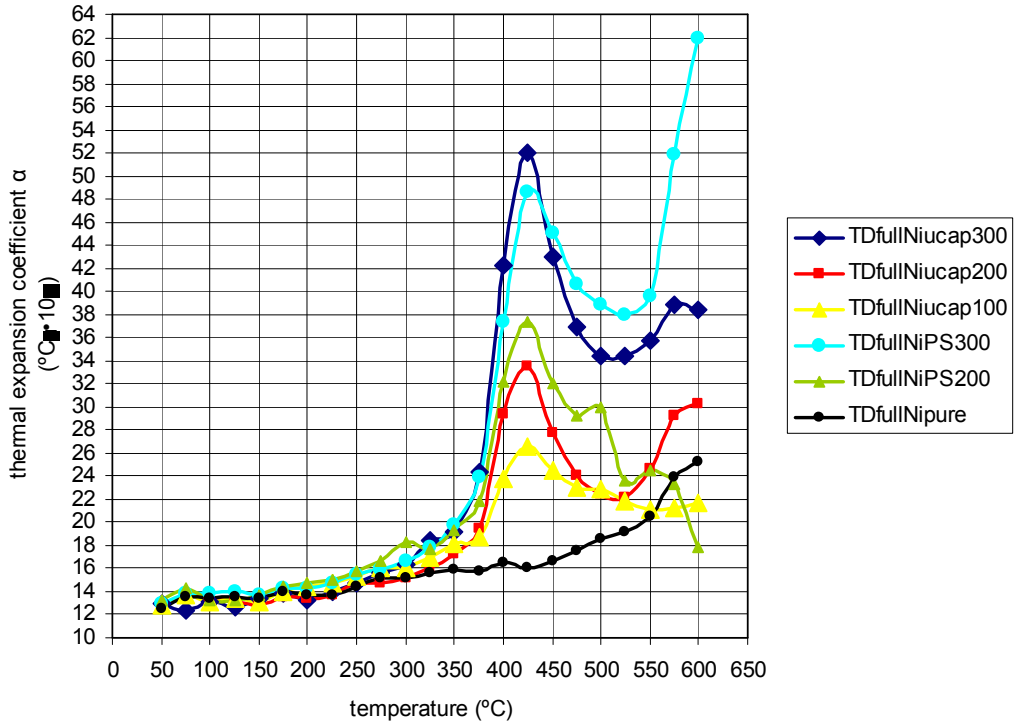

Figure 4.22 Variation of the thermal expansion coefficients of nickel coatings with temperature

Observing figure 4.22, it is noticed that coatings containing different amount of microcapsules have almost parallel curves. In the case of coatings containing PS particles, the effect is similar except a small peak at 500 ºC and the descending slope from 550 ºC on in the case of NiPS200.

When studying their potential applicability as thermo actuators, all samples have a sharp thermal expansion coefficient increase in the temperature range from 350 ºC to 425 ºC followed by a remarkable reduction from 425 ºC to 525 ºC.

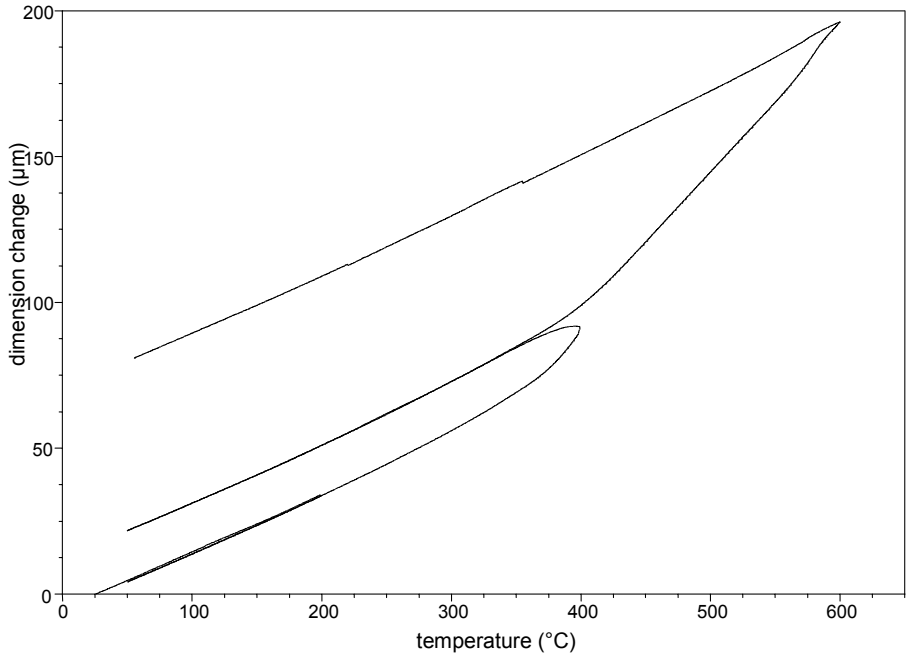

Figure 4.23 Dimension change during the partial heating cycles from room temperature to 200 ºC, 50-400 ºC and 50-600 ºC of a nickel coating containing 100 g/l (5.5 %vol) microcapsules. Heating rate: 3 ºC/min from room temperature to 200 ºC in the first cycle, from 50 ºC to 400 ºC in the second and from 50 ºC to 600 ºC in the third cycle maintaining both extreme temperatures (50, 200, 400 and 600 ºC) during 2 minutes (isothermal). Argon atmosphere. Initial length: Niucap100 (13.9485 mm)

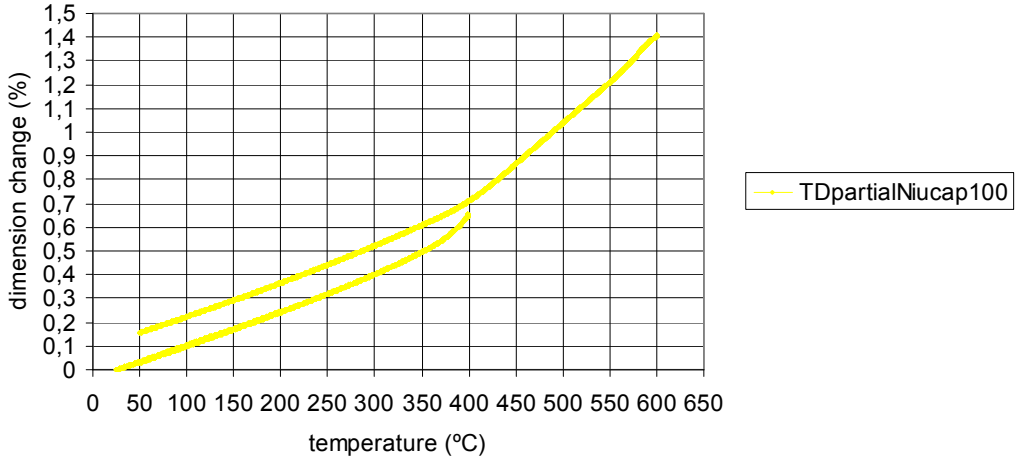

Figure 4.24 Dimension change in percentage versus temperature of a nickel coating containing 100 g/l (5.5 %vol) of microcapsules during a partial cycling test

During the first partial cycling from room temperature to 200 ºC of the nickel coating containing 100 g/l (5.5 %vol) of microcapsules, the expansion provoked by the thermal load is completely elastic as it is recovered during the cooling cycle.
After the second cycle from 50 ºC to 400 ºC some plastic deformation is obtained as the water contained inside the microcapsules has evaporated in part. This effect is evident after reaching 350 ºC, with an increase in the curve slope.

In the third heating cycle from 50 ºC to 600 ºC, the curve has two different slopes, one lower below 375 ºC and other sharper from 375 ºC on because of the increase in pressure due to the complete evaporation of water.

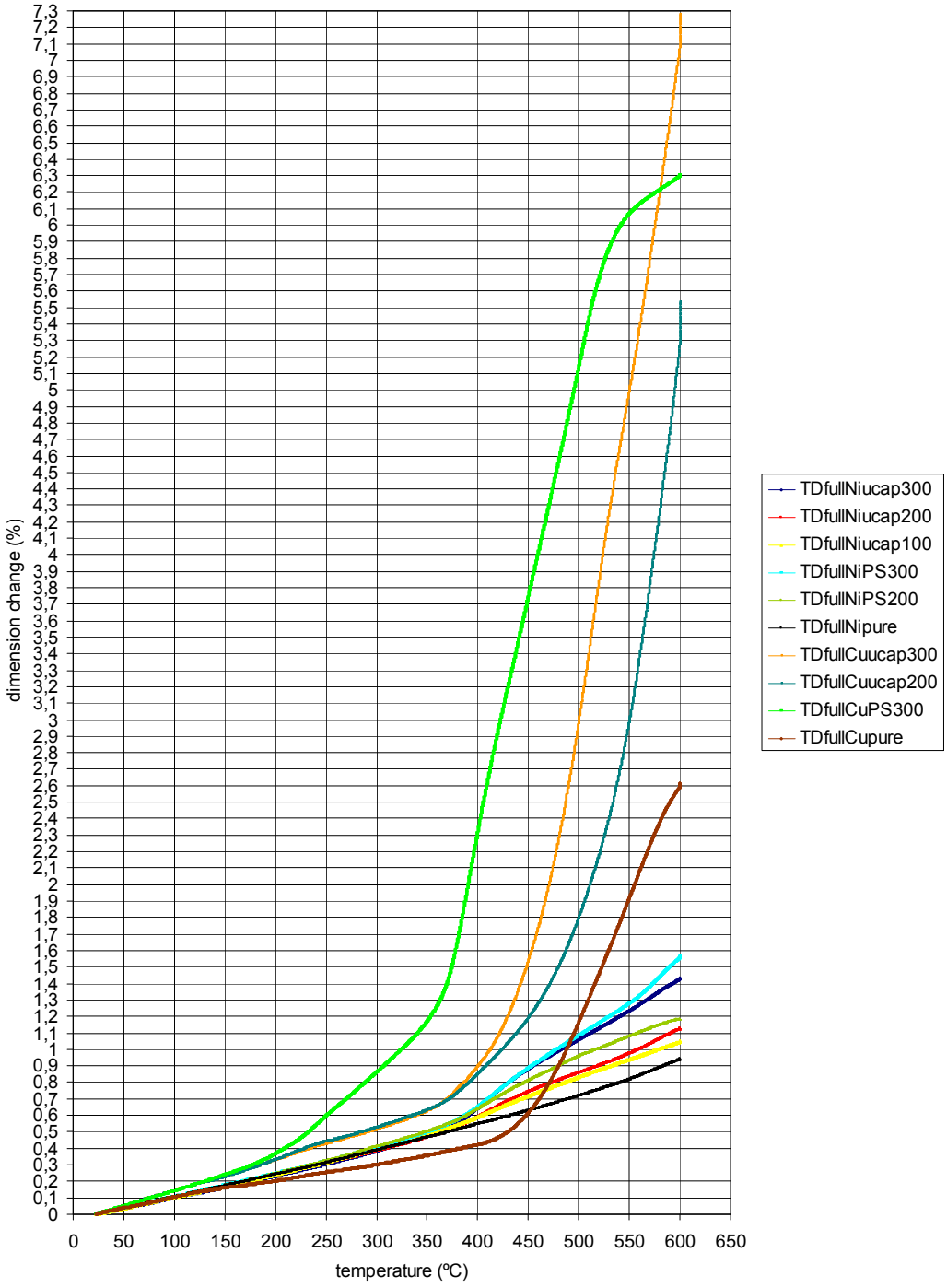

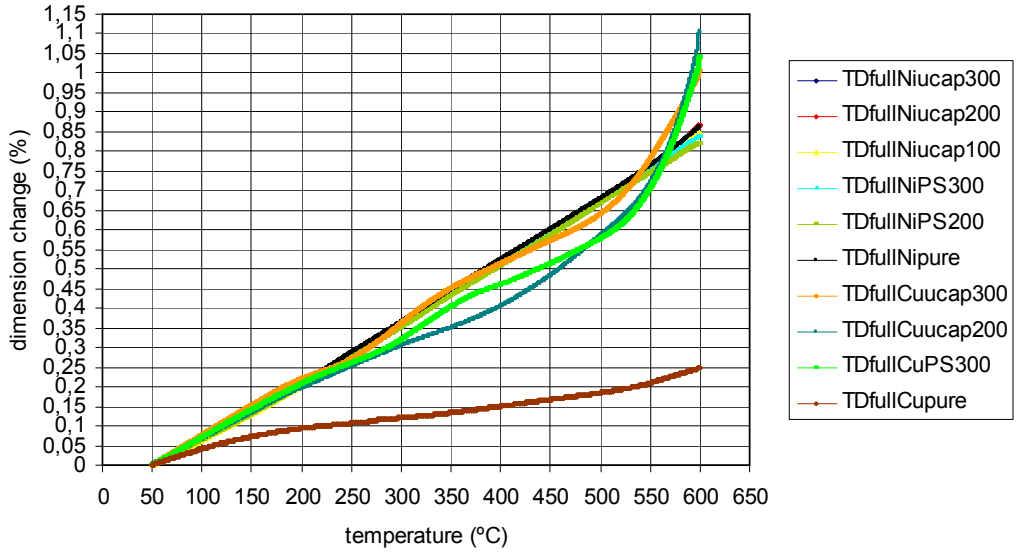

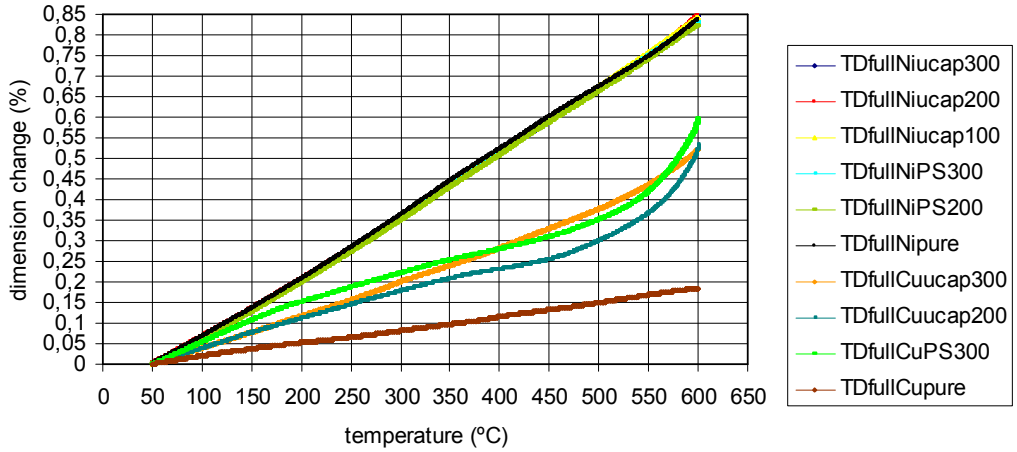

Figures 4.25, 4.26, 4.27 Comparative of the three heating cycles between all the samples after full cycling

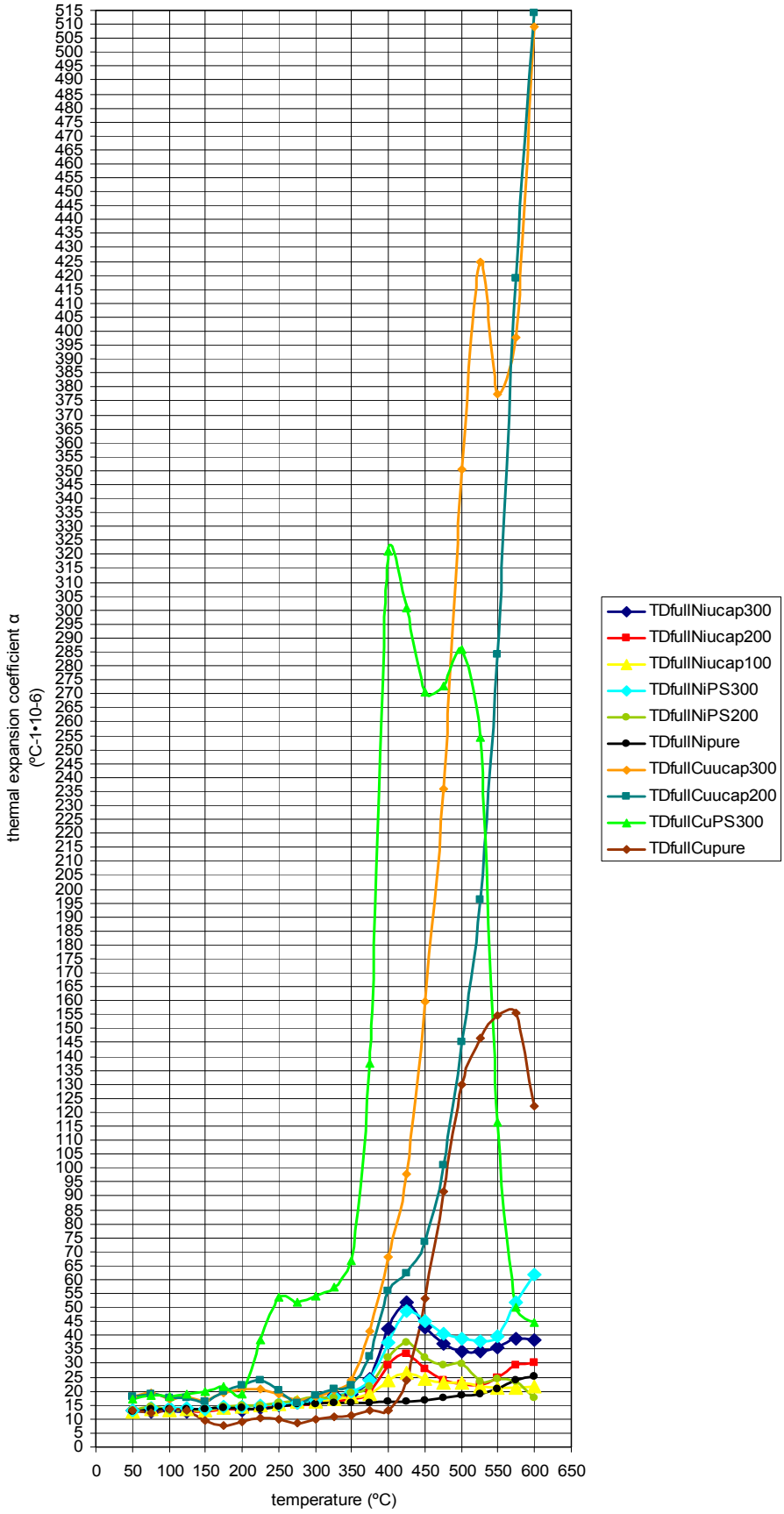

Figure 4.28 Variation of the thermal expansion coefficients of all the samples with the temperature

4.1.3 Results analysis

The obtained results of the thermal dilatometry show the dependence of the samples on the mechanical and thermal properties of both the metal matrix and the particles embedded on it.

First of all, it is evident in both types of copper and nickel coatings containing microcapsules that no sharp rise in thermal expansion is observed at the water boiling point (100 ºC). On the other hand, the non-linear increment starts at around 400 ºC in both cases as shown in Figure 4.25. This behaviour is produced because of the thermal expansion difference between the metal matrix and the embedded microcapsules, appearing thermal stresses in the composites.

In order to explain this process in detail, the equation of Classius-Clapeyron must be used.

$$\frac{dp}{dT} = \frac{L_v}{T(V_v - V_l)} \tag{4.2}$$

With T the absolute temperature, dp the differential variation in vapour pressure due to a differential temperature change, V_v - V_l volume variation per mole when water evaporates and L_v latent heat of vaporisation per mole.

The water contained inside the embedded microcapsules will evaporate as the temperature differential increases and it will provoke a consequent pressure differential increment. According to the phase diagram of water, the next differential volume of water will boil at higher temperature. This phenomenon will continue until all the water is evaporated, giving as a result a boiling trajectory instead of just a single boiling point.

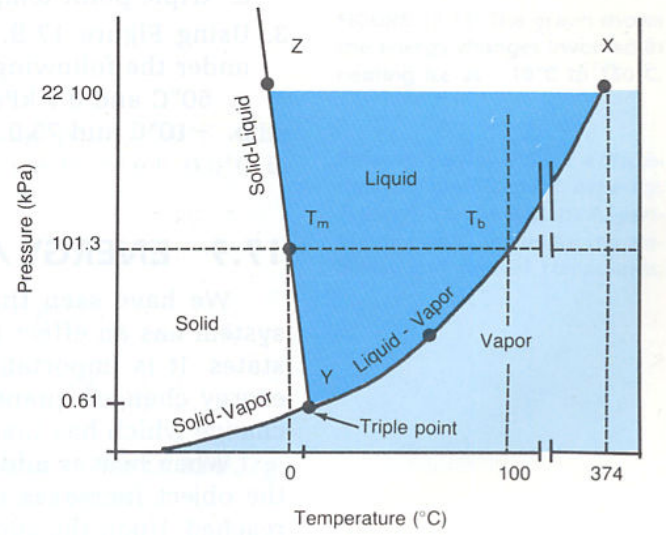

Figure 4.29 Pressure-temperature phase diagram of water

This boiling trajectory explains why no first-order transition appears at the water boiling point in the thermal expansion curves (Figure 4.25). The sharp rise in thermal expansion starts at 375 ºC in the case of copper samples because of the vapour pressure. From that point on, the expansion behaves linearly with a pronounced slope. In the meanwhile, in nickel samples containing microcapsules, the rise in thermal expansion is much smoother and occurs between 375 and 450 ºC.

After all the water of the microcapsules is vaporised, the resultant vapour is studied as an ideal gas following the law:

$$pV = nRT \tag{4.3}$$

where p is the gas pressure, V is the gas volume, R is the gas constant (8.314J/mol·K) and T is the absolute temperature.

As the metal matrix is plastically deformed during the first expansion and it does not recover its original shape after the thermal stresses are relieved, the matrix holes in which the microcapsules were embedded are now bigger than before. Therefore, during the following heating cycles, the gas pressure is not high enough to increment the plastic deformation in the same quantity as the first cycle. As a result, the thermal expansion is smaller during the second cycle and it is even smaller during the third one.

In order to describe the thermal expansion of composites containing spherical particles embedded in their matrix, the micromechanical model of Bullough and Davis[10] is used. In this model, each spherical particle of radius a is assumed to be embedded in a spherical matrix of radius b. The volume fraction of particles contained in the samples is f.

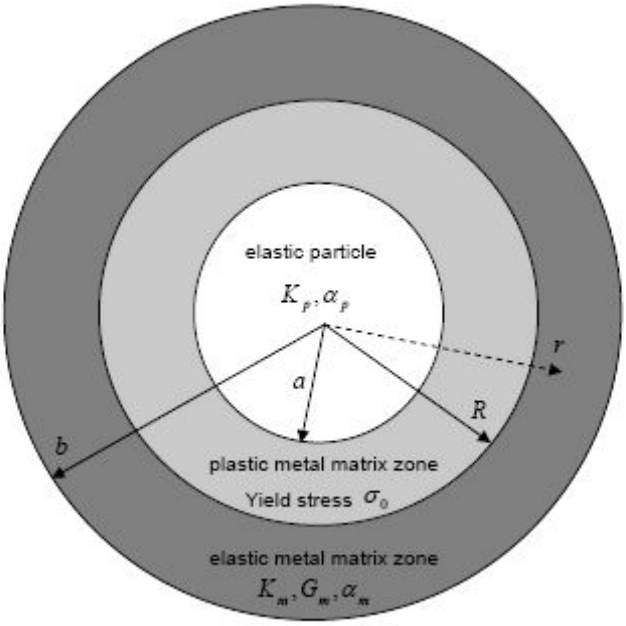

Figure 4.30 The metal matrix volume in the region $a \leq r \leq R$ deforms plastically, while the volume in the regions $r < a$ and $R < r \leq b$ remains elastic

This model allows working with spherical coordinates giving a complete analytical formulation for the hydrostatic stress in the particle. However, it has some limitations due to the assumption of the spherical geometry: spheres do not fill the whole space and the model does not take into account the interactions between particles.

During the tests, temperature is assumed to vary slowly enough (rate 3 ºC/min) leading in a uniform temperature distribution in the matrix and the particle. During the heating, the mismatch between the thermal expansion of the matrix and the particle provokes thermal stresses. As the particle experiments a larger expansion than the metal matrix does, it will lead into pressure over the particle:

$$P_p = \frac{12(1-f)K_p K_m G_m(\alpha_m - \alpha_p)\Delta T}{4G_m(K_p - K_m)f + K_m(3K_p + 4G_m)} \tag{4.4}$$

with K_m and G_m the bulk and shear modulus of the metal matrix, K_p the bulk modulus of the particle and α_m and α_p the thermal expansion coefficient of the matrix and the particle and f the volume fraction of particles embedded in the matrix.

Table 4.3 Pure metal and particles mechanical and thermal properties

	copper	nickel	polystyrene
density ρ (kg/m^3)	8960	8910	1050 (solid) 900 (liquid)
melting temperature T_m (ºC)	1083	1453	-
thermal expansion α at 25 ºC (ºC^{-1}·10^{-6})	16.5	13.4	90
thermal conductivity k at 25 ºC (W/m·K)	398	90	0.13
thermal storage capacity c (J/kg·K)	386	443	1170
elastic modulus E (GPa)	115	207	2.28-3.28
yield stress σ_0 (MPa)	18-69	35-107	-
Poisson's ratio v	0.34	0.31	0.33
shear modulus G (GPa)	46	76	-
bulk modulus K (GPa)	115	182	2.24-3.22

Those thermal stresses have the following formulates for the radial and the tangential cases:

$$\sigma_r(r) = \frac{f}{1-f}\left(1-\frac{b^3}{r^3}\right)P_p \tag{4.5}$$

$$\sigma_t(r) = \frac{f}{1-f}\left(1+\frac{b^3}{2r^3}\right)P_p \tag{4.6}$$

The displacement in the matrix during the thermal expansion is given by:

$$u(r) = \frac{4G_m(K_p\alpha_p - K_m\alpha_m)f + K_m\alpha_m(3K_p+4G_m)}{4G_m(K_p-K_m)f + K_m(3K_p+4G_m)}(T-T_0)r - \\ -\frac{3K_mK_p(\alpha_m-\alpha_p)}{4G_m(K_p-K_m)f + K_m(3K_p+4G_m)}(T-T_0)\frac{a^3}{r^2} \tag{4.7}$$

The thermal expansion α of the composite can be calculated by substituting the displacement of the matrix in b in the equation of the linear expansion:

$$\alpha = \frac{1}{L}\frac{dL}{dT} = \frac{1}{b}\frac{du(b)}{dT} \tag{4.8}$$

However, these equations are only valid in case of a spherical particle in a linear isotropic elastic matrix which is not our case as copper and nickel coatings suffer plastic deformation during thermal expansion. Therefore, this micromechanical model must be simplified and adapted to these composites by making some assumptions:[11]

- The microcapsule's wall is thin enough to be neglected
- There is no initial space between particles and matrix at room temperature
- The temperature is uniform across matrix and particle

- The non-ideally plastic deformation of pure copper is described by an exponential power law whereas nickel exhibits linear plastic deformation

  The exponential power law applied to copper expansion behaviour replaces its actual mechanical properties by a quasi-elastic shear modulus G_{Cu}:

$$G_{Cu} = \frac{1}{3}\frac{\partial \sigma_{Cu}}{\partial \varepsilon_{Cu}} = \sigma_K \frac{n\varepsilon_{Cu}^{n-1}}{\varepsilon_K} \exp\left(-\frac{\varepsilon_{Cu}^{n}}{\varepsilon_K}\right) \tag{4.9}$$

  where σ_{Cu} and ε_{Cu} are the stress and strain of copper and σ_K and ε_K are temperature dependent constants and n is an exponential factor.

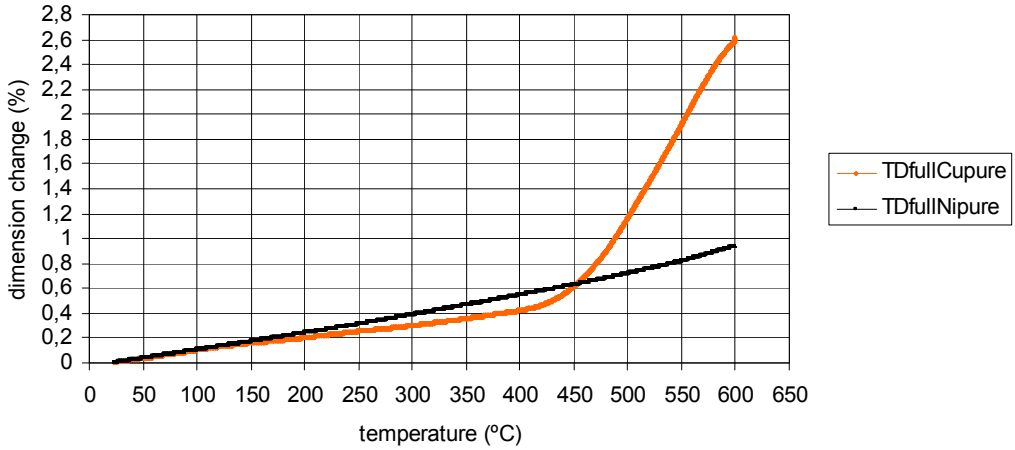

Figure 4.31 Comparison between deformation of pure copper and nickel coatings when heating from room temperature to 600 ºC with a heating rate of 3 ºC/min in argon atmosphere

- The thermal and mechanical properties of the sphere formed by the microcapsule and the surrounding matrix will be homogenized by a weighed average as both are volume elements with different properties, elastic versus plastic behaviour for the matrix and solid versus liquid state for the microcapsule.

The behaviour of samples during experiments is completely different depending on which heating cycle is running. After the first heating cycle, the matrix holes have been deformed plastically and in subsequent cycles the microcapsules can expand provoking mainly elastic deformation and much less plastic deformation. This elastic deformation is larger in the case of nickel coatings thanks to their bigger Young modulus, 115 GPa for copper and 207 GPa for nickel. As the sample is being heated, the pressure on the microcapsule / PS particle is increased and this causes a boiling / melting trajectory instead of a single point.

At the same time, the metal matrix expands elastically under the thermal loads until the Von Mises stress is passed at the interface matrix – particle. From that point on, the metal matrix volume in the region $a \le r \le R$ deforms plastically, while the one contained in the region $R < r \le b$ remains elastic. This is shown in the previous Figure 4.30.

As the radial stress (equation 4.5) decreases rapidly with the radius r, the plastic deformation is mainly caused by the tangential stress (equation 4.6). The average value of the tangential stress in the plastic region $a \le r \le R$ is given by the expression:

$$\overline{\sigma}_t = \frac{f}{1-f}\left\{R\left[1-\left(\frac{b}{R}\right)^3\right] - a\left[1-\frac{1}{4f}\right]\right\}P_p \tag{4.10}$$

In order to obtain the quasi-elastic modulus of the matrix for the plastic region, this value is substituted in the equation 4.9.

The radius R, which is the interface between the elastic and plastic regions, is calculated assuming Von Mises stress is reached:

$$R = \left(\frac{fP_p}{2(1-f)\sigma_0} \right)^{\frac{1}{3}} b \tag{4.11}$$

By using the previous equations, now it is possible to calculate the thermal strain and the expansion coefficient as function of it.

$$\varepsilon_t = \frac{u(b)}{b} \tag{4.12}$$

$$\alpha = \frac{\varepsilon_t}{\Delta T} \tag{4.13}$$

After the first heating cycle, the deformation obtained will be mainly elastic because the holes provoked in the first cycle are larger than the particles sizes.

This effect can be appreciated in the following cross sections micrographs taken after the thermal cycles.

4.1.4 Samples cross section micrographs after thermal dilatometry

Micrographs are taken by using an optical microscope applying a magnification of 32x in all the samples studied.

During heating, the particles degrade and diffusion processes occur, leading to dendrites and big holes in the case of partial cycling. For full cycling samples, the transformation is much deeper and some of the samples had scales after performing the test.

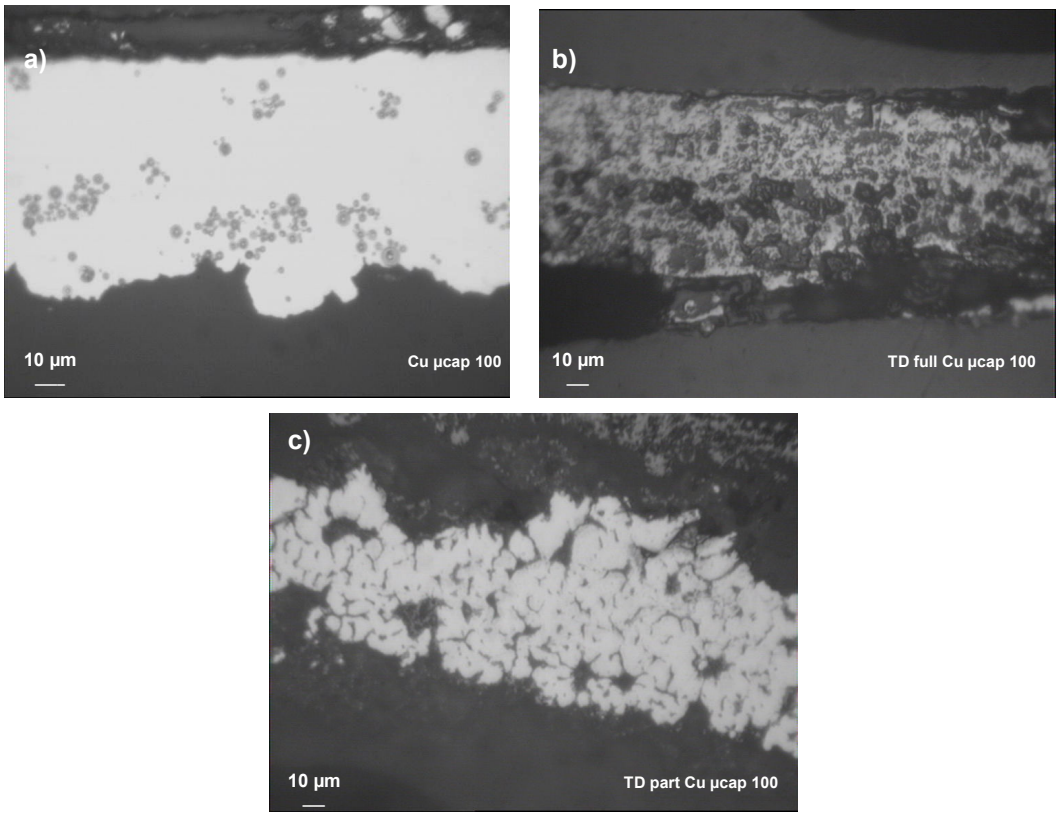

Figure 4.30 Pictures comparing the microstructures of copper samples containing 100g/l of microcapsules before (a) and after full (b) or partial (c) cycling thermal dilatometry

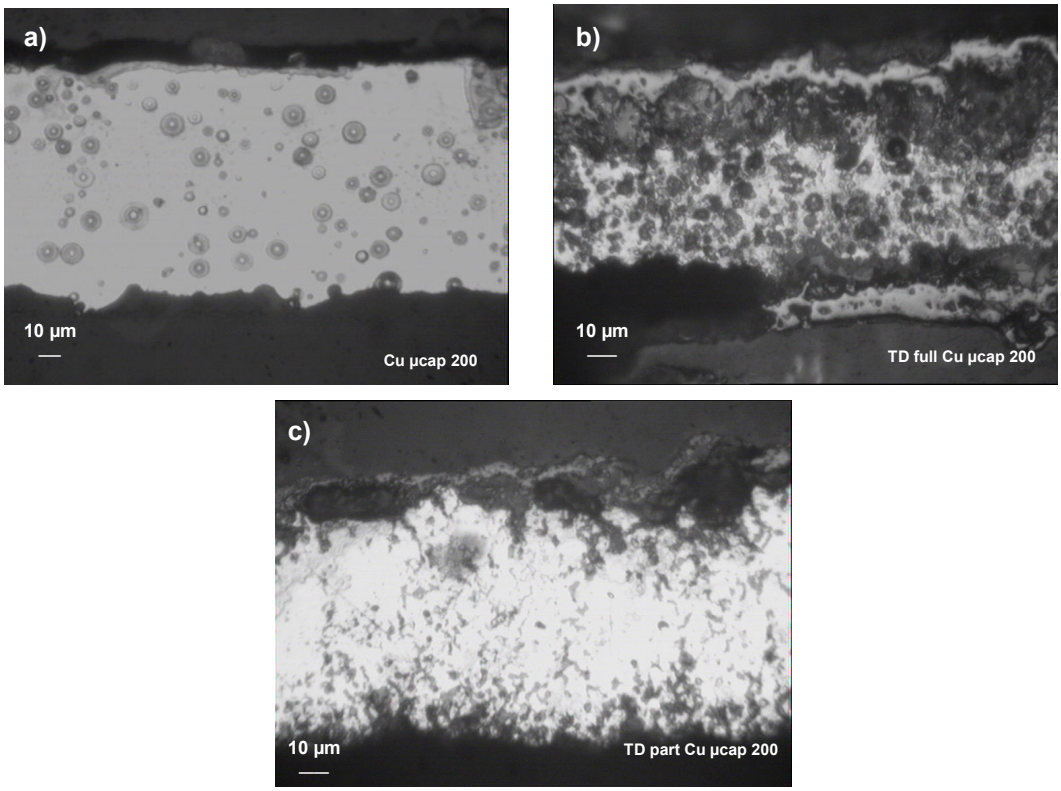

Figure 4.31 Pictures comparing the microstructures of copper samples containing 200g/l of microcapsules before (a) and after full (b) or partial (c) cycling thermal dilatometry

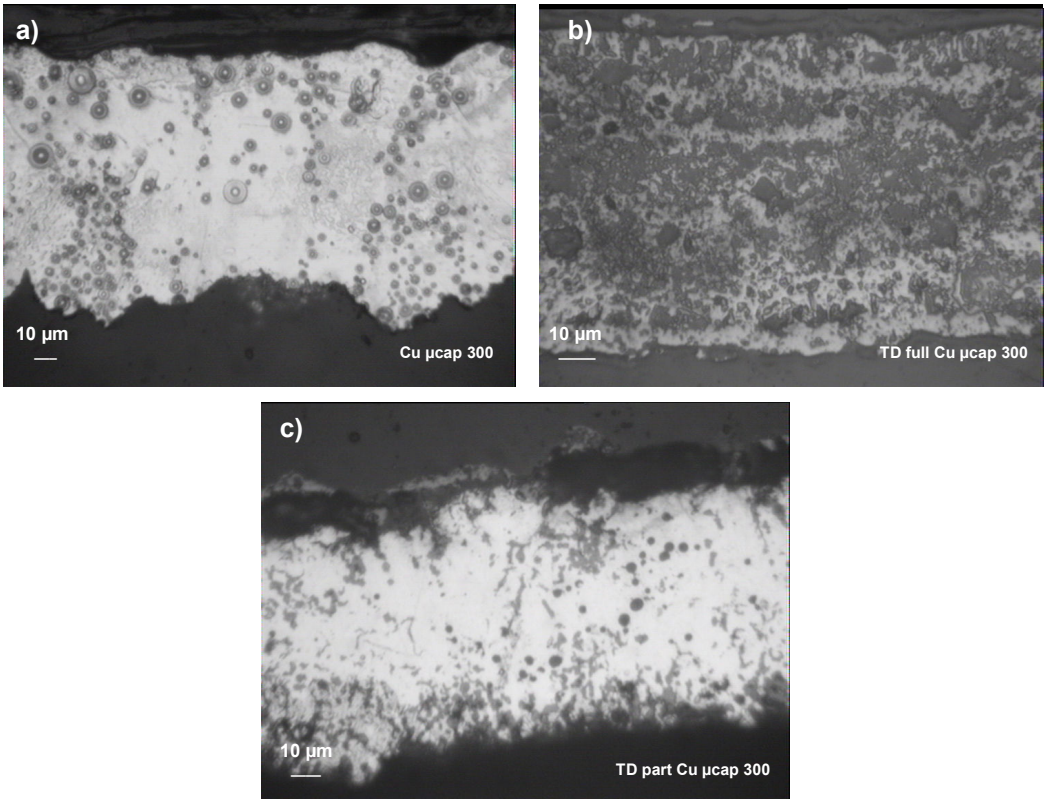

Figure 4.32 Pictures comparing the microstructures of copper samples containing 300g/l of microcapsules before (a) and after full (b) or partial (c) cycling thermal dilatometry

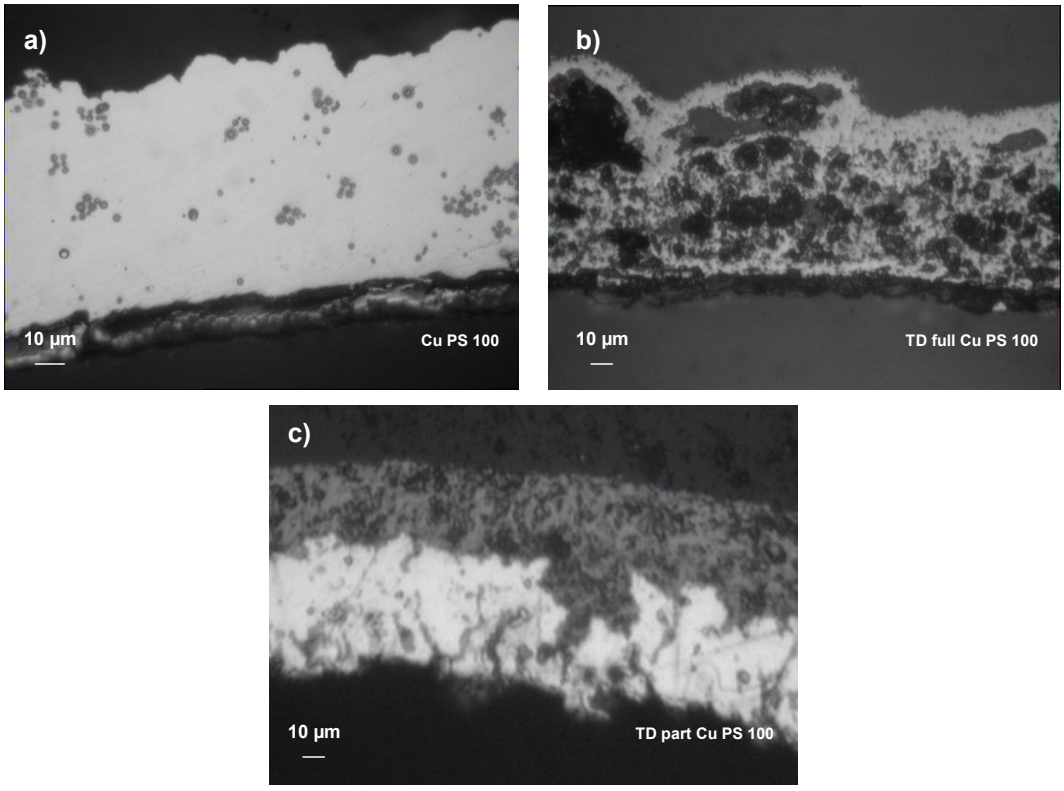

Figure 4.33 Pictures comparing the microstructures of copper samples containing 100g/l of PS particles before (a) and after full (b) or partial (c) cycling thermal dilatometry

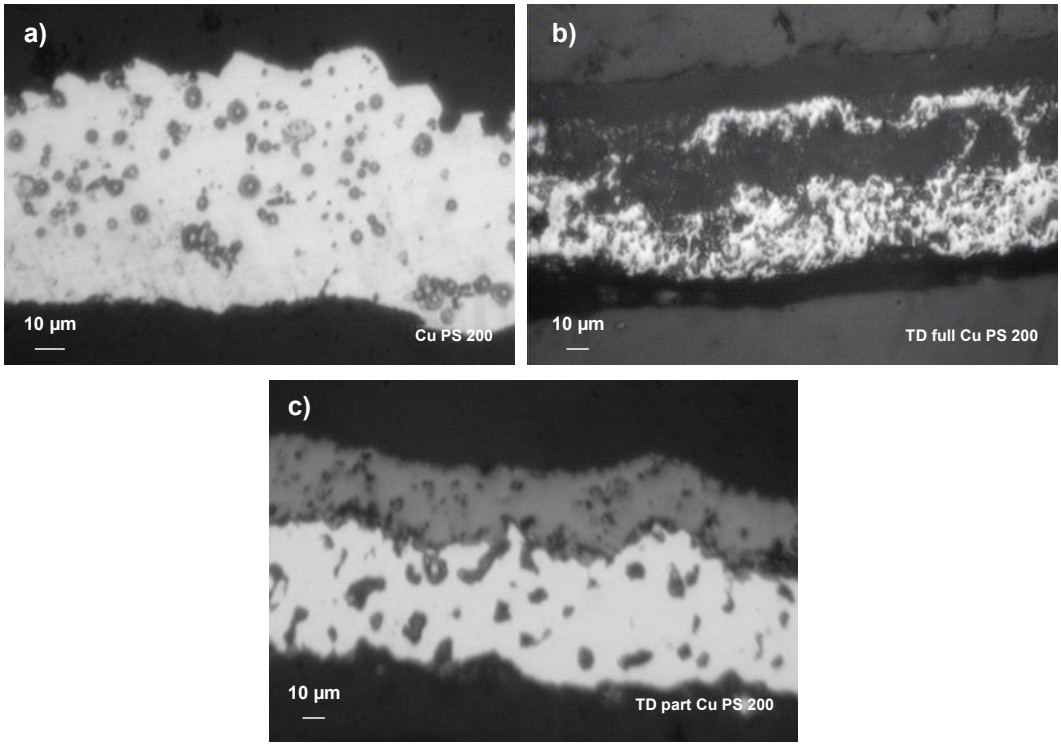

Figure 4.34 Pictures comparing the microstructures of copper samples containing 200g/l of PS particles before (a) and after full (b) or partial (c) cycling thermal dilatometry

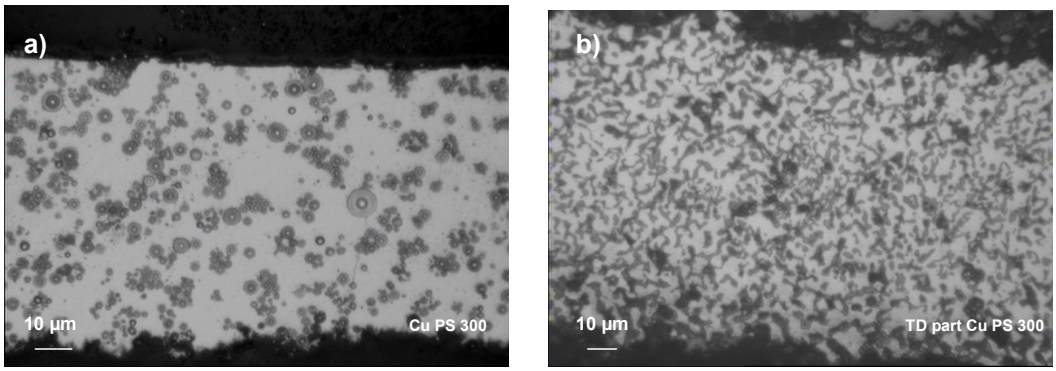

Figure 4.35 Pictures comparing the microstructures of copper samples containing 300g/l of PS particles before (a) and after partial (b) cycling thermal dilatometry

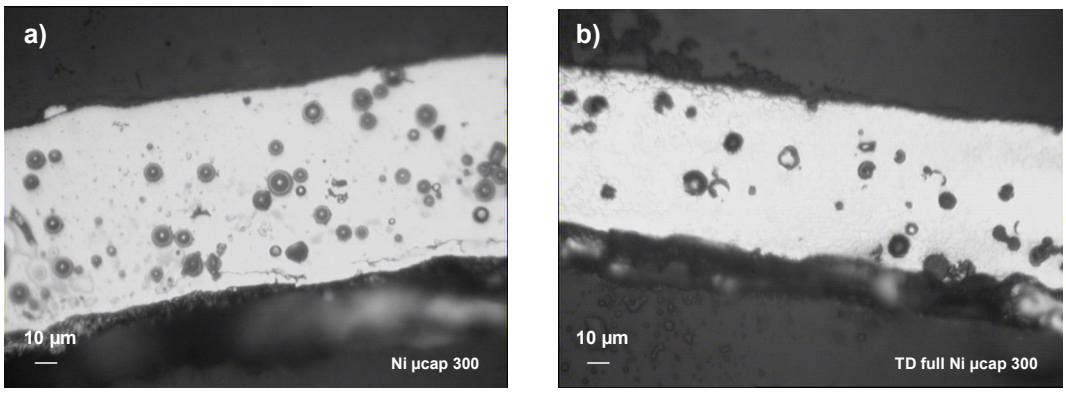

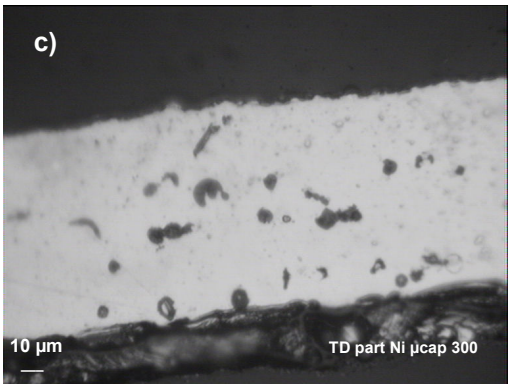

Figure 4.36 Pictures comparing the microstructures of nickel samples containing 300g/l of microcapsules before (a) and after full (b) or partial (c) cycling thermal dilatometry

Chapter 5: *Conclusions*

The present work consists in the development and testing of copper and nickel coatings produced by electrodeposition containing microcapsules with water as core material and solid polystyrene particles. It has been studied its applicability as thermo actuator materials with high thermal expansion coefficients and therefore, a fast response time in small temperatures ranges.

When performing the differential scanning calorimetry (DSC) test on samples, in the case of coatings with microcapsules containing water, it is observed a boiling trajectory in a wide temperature range starting at 200 ºC. That produces a sharp deformation at 375 ºC due to the pressure ejected by the vapour.

In the case of coatings with PS particles, the degradation of the polymer starts at 400 ºC after the reorganization of its chains. This value coincides with the theoretical one because copper matrix expands under the thermal load and diminishes the pressure over the particles.

The results obtained after applying the thermal dilatometry test (TD), show several temperatures ranges for the different coatings where the thermal expansion coefficient increases sharply, provoking a strong expansion (or compression in the case of Ni coatings at high temperatures). This characteristic would allow the using of the studied materials as thermoactuators.

The lower the stiffness of the material, the higher the thermal deformation produced. As a result, copper coatings suffer higher thermal deformations than nickel ones.

It is also clear that coatings containing PS particles start their expansion at lower temperatures with sharper slopes, although coatings containing microcapsules reach higher thermal expansions.

However, during subsequent cycles, the deformation obtained is much lower and mainly elastic. That is why, the use of these materials would be restricted and once used they should be replaced.

References

1974 [1] W.H. SAFRANEK, "The properties of electrodeposited metals" Elsevier Publishing

2001 [2] CALLISTER W.D., "Fundamentals of material science and engineering" 5th edition, chapters 7th and 17th

2007 [3] QINGWEN S., YI L., JIANWEI X., HU J.Y., YUEN M., "Thermal stability of composite phase change material microcapsules incorporated with silver nano-particles", Polymer 48 3317-3323 (2007)

2006 [4] ZHENZHEN LI, FRANSAER J., "Metal-liquid composite coatings for thermal actuators"

2007 [5] SARIER N., ONDER E., "The manufacture of microencapsulated phase change materials suitable for the design of thermally enhanced fabrics", Thermochimica acta 452 146-160 (2007)

[6] STOJAK J.L., FRANSAER J., TALBOT J.B., "Review of electrodeposition" p193-221

[7] www.mastersizer.com

2001 [8] FARAVELLI T., PINCIROLI M., PISANO F., BOZZANO G., "Termal degradation of polystyrene", Journal of analytical and applied pyrolysis 60 103-121 (2001)

2007 [9] AHMAD Z., AL-AWADI N.A., AL-SAGHEER F., "Morphology, thermal stability and visco-elastic properties of polystyrene-poly (vinyl chloride) blends", Polymer degradation and stability 92 1025-1033 (2007)

1995 [10] BULLOUGH R., DAVIS L. C., "The residual deformation fields in particle reinforced metal-matrix composites", Acta metallurgica Vol. 43 No 7 p2737-2742 (1995)

2006 [11] MALFLIET A., DEFERME G., STAPPERS L., FRANSAER J., "Synthesis and characterization of composite coatings for thermal actuation", Journal of the Electrochemical Society, 154 (1) D50-D56 (2007)